The Role of Cooperation and Dispersal in the Evolution of Antibiotic Resistance

by

Tatiana Artemova,

B.S., Moscow Institute of Physics and Technology (2009)

Submitted to the Department of Physics
in Partial Fulfillment of the Requirements for the Degree of

Doctor of Philosophy in Physics
at the

MASSACHUSETTS INSTITUTE OF TECHNOLOGY

June 2015

Signature redacted

Signature of Author .....
Department of Physics
May 18, 2015

Signature redacted

Certified by .....
Jeff Gore
Professor of Physics
Thesis Supervisor

Signature redacted

Accepted by.....
Nergis Mavalvala
Associate Department Head for Education

The Role of Cooperation and Dispersal in the Evolution of Antibiotic Resistance

by

Tatiana Artemova,

Submitted to the Department of Physics
on May 21, 2015, in partial fulfillment of the
requirements for the degree of
Doctor of Philosophy in Physics

Abstract

Understanding mechanisms of evolution under in real biological systems is a fundamental problem. Natural selection is one of the mechanisms that drive evolution. Due to the natural selection, phenotypes with higher fitness than the rest of the population increase in frequency and eventually dominate the populations. In real biological systems due to interactions between individuals within a population, it is not always obvious how natural selection manifests itself. Here we consider two types of interactions – cooperative antibiotic break down and spatially expanding populations. In each of the cases predicting which phenotype is the most fit and the patterns corresponding to selection of this phenotype could be not straightforward.

(1) Bacterial antibiotic resistance is typically quantified by the minimum inhibitory concentration (MIC), which is defined as the minimal concentration of antibiotic that inhibits bacterial growth starting from a standard cell density. However, when antibiotic resistance is mediated by degradation, the collective inactivation of antibiotic by the bacterial population causes the measured MIC to depend strongly on the initial cell density. Given this dependence, the relationship between MIC and bacterial fitness in such cases is not well-defined. Here we demonstrate that the resistance of a single, isolated cell—which we call the single cell MIC (scMIC)—provides a superior metric for quantifying antibiotic resistance. Unlike the MIC, we find that the scMIC predicts the direction of selection and also specifies the antibiotic concentration at which selection begins to favor new mutants. Understanding the cooperative nature of bacterial growth in antibiotics is therefore essential in predicting the evolution of antibiotic resistance.
(2) During the expansions of natural populations, new phenotype can emerge. If it is fitter than the rest of the population, it will take over. However, the exact spatial patterns of this process are unknown. Here we show that for a wide class of models the fraction of the fit mutant should increase exponentially. We also observe this pattern experimentally by observing bacterial populations expanding in soft agar, as well as connection between the steepness of the exponent to the fitness difference.

Thesis Supervisor: Jeff Gore

Title: Professor of Physics

Acknowledgements

I would like to thank my PhD advisor Jeff Gore for teaching me how to do research, for being a good mentor, and, above all, for always being very supportive and encouraging. Jeff is one of the very few people who can provide guidance in any aspect of life, who can transmit passion and recharge other people with energy, and who can make people around him eager to explore opportunities and be active. I would also like to thank Jeff for sharing and demonstrating the wisdom that active involvement in creating something new is very often much better than passive exploration of the subject. Jeff has been a great role model for me both professionally and personally.

I would like to thank all members of the Gore lab. I am fortunate for having had the opportunity to share ideas and many experiences with you over the years. The lab has often been a great source of friendship and comfort for me.

I would like to thank my thesis committee members – Professor Mirny and Professor Weinberg for giving valuable input to this work.

Finally, I would like to thank my friends and family without whose love and support I would have never been able to get through any of the difficulties. I would like to thank my father for teaching me to be persistent and for making my education a great priority. I would like to thank my mother for providing unconditional love and support and for always being available when I need her. She has also been a great role model of an ambitious independent woman with many interests.

Chapter 1. Introduction

In the second half of the nineteenth century Charles Darwin published "On the origin of species". Since then there have been many studies exploring how natural populations evolve over time. In contemporary interpretations of evolutionary theory, this is quantified by how the allele (i.e. specific version of a gene) composition of population depends on time, and the functional form of this dependence is shaped by several fundamental processes. Some of these processes have deterministic outcomes and others are stochastic in nature. The approach to biological systems that seeks to understand these processes and their outcomes and confirm their relevance in natural populations is similar physicists' approach of finding laws governing matter and the universe.

One important mechanism of evolution introduced by Darwin is natural selection. It will play an important role in both research projects described in this thesis. Since this thesis includes physicists as a target audience, I will briefly introduce natural selection below. Natural selection is a process that eventually assigns higher probabilities of survival to the individuals with higher fitness. Every individual has a fitness that is a measure of reproductive ability – the more an individual is likely to pass its genes to descendants, the higher the fitness. Fitness is a function of the environment the individual is put in – it is possible (and often happens) that in one environment individual A is more fit than individual B, and in another environment individual B is more fit than individual A. The word 'environment' is used in a general sense: it could be temperature, humidity, as well as presence or absence of certain food sources, individuals of the same or different species or even a previous history of the lineage in question.

The problem of the outcome of natural selection is reduced then to the problem of defining fitness of each individual in a given environment, and then predicting the outcome of the natural selection is trivial: the fittest wins (at least when stochastic effects can be neglected). This is why there has recently been a significant body of research studying fitness landscapes that map genotypes or phenotypes to fitness(Weinreich *et al*, 2006)(Tan *et al*, 2011). These studies often do high-throughput data processing to answer the questions of what are the possibilities of a given organism to increase its fitness through the

process of mutation, which is another important process in evolution theory that creates the variation which is necessary for selection to be effective. While fitness can be measured though competition with some reference strain, in practice it involves tagging all the strains which complicates the process. Usually some characteristic of the growth process without direct competition is used as a proxy for fitness, but different characteristic should be used in different environments.

To study evolution in the lab, microbial populations are commonly used for several reasons. First of all, usually, the smaller and simpler organism is, the smaller is its generation time. Reproductive advantage (or disadvantage) can only manifest itself on time scales much larger than the generation time. Therefore, to make experiments in the lab feasible for incremental hypothesis testing, it is important to work with the organisms that reproduce fast.

Second, microorganisms tend to have small genomes as compared to large animals. For example, the genome size of the bacterium *E. Coli* is 4.6 million base pairs, the genome size of the budding yeast *S. cerevisiae* is 12.2 million base pairs, and for comparison, the human genome is 3.2 billion base pairs. The microorganisms mentioned above have not only been sequenced, their genes have been identified and, for many of them, their function is understood.

Third, the organisms themselves and the experimental procedures on them are relatively simple. The organization of the interaction with the nutrients in the media is quite simple as compared to the mammals, for example. Microbes do not have a nervous system, for example, which makes their responses to the environment simpler and therefore easily interpretable.

Fourth, which is really combining the second and third point: microbial organisms are relatively amenable to genetic manipulation. The bacterium *E. coli*, for example, is able to carry plasmids (extra pieces of cicular DNA), which can be put inside a given lineage within hours. It is also possible, using microbiological techniques, to insert a gene in a plasmid. Therefore, bacteria can be relatively easily made

to carry a certain gene. This is all very important for evolutionary studies because identifying the influence of a given mutation can often require some artificial engineering of a mutant.

One very prominent example of experimental evolution of microbes is an ongoing long-term evolution experiment by R. Lenski started in 1988. With over than 60000 generations of *E. coli* the researchers are still observing an increase in fitness, suggesting that the fitness can be increased essentially without bound(Wiser *et al*, 2013). This is an interesting and not obvious result. There are also many other conclusions that have been made from the data, some of which are hoped to be universal statements about evolution and not specific to *E. coli* in the environment they use(Barrick & Lenski, 2013). Therefore, evolution of microbes in the laboratory is useful for discovering general principles of evolution that can afterwards be tested on other organisms or in other conditions to verify the generality.

In the research projects presented in this document we also use *E coli* as a model organism. *E coli* is a single-celled prokaryotic organism, rod shaped, a few micrometers in length and 1 micrometer in diameter. Most *E. coli* strains do not cause disease in humans, but some of the strains can cause diseases such as urinary tract infections, gastroenteritis, to which antibiotics are usually used as a treatment. In this document, we often grow bacteria *E. coli* in an antibiotic environment. Therefore, fitness most of all depends on antibiotic concentration and the ability of bacteria to tolerate a given antibiotic concentrations.

We use the described experimental system to study evolution. It is essential that in order for natural selection to act, there should be some variation in genes, i.e. diversity. Therefore, the population should have some number of individuals that is greater than one. Realistically, for bacteria it is usually population sizes of millions and tens of millions within a centimeter distance from each other. Inevitably, at such densities, bacteria interact with each other. The interaction usually happens through release of a chemical that other bacteria can sense and sometimes even genetic material (plasmids) can be released, and other bacteria can accept it and incorporate it into their genomes. The released chemicals can make

life of other individuals better, worse or not influence their fitness. When the life of the consumer of the chemical becomes better, the interaction is called cooperation.

Cooperation in nature can be challenging to understand. After all, production of the chemicals is costly since it requires resources that otherwise could be used to increase reproduction rate and therefore decreases fitness of the producing individual somewhat. On the other hand, the acceptor of the chemical benefits from it in some way, which means that its fitness is increased. Therefore, through natural selection, the producer of the public goods should become extinct because it has lower fitness as compared to identical individual who do not produce this public good.

There are many examples of cooperation in nature. The social organization of ants colonies, bee swarms and wasp nests lets very few individual reproduce, while other individuals produce and provide resources that makes the reproduction of the selected individual possible. While at first glance it may seem that nonproducing individuals should become extinct through the process of natural selection, the selection acting on the genes makes the genes of even non-reproducing individuals pass to the next generation, a selection type called kin selection. Also any multicellular organism (human for example) can be considered as a cooperative system of its cells.

Cooperation has been studied extensively both theoretically and experimentally in the lab(Axelrod & Hamilton, 1981)(Nowak, 2006)(Gore *et al*, 2009). Various theories and experimental designs seek to understand under which conditions can cooperation emerge and when and why the so called free riders—who do not cooperate—dominate the system and destroy cooperation. A game theoretical approach is a very common way to conceptualize benefits and costs for a unit that selection acts on. Microbes and viruses are usual organisms to test the analysis generated by these models and to gain new insights into many ways in which cooperation manifests itself in the real world.

While it is interesting to understand how cooperation emerges, it is a fact of life: it exists. It makes studying cooperative systems complicated because the population is not anymore a set of identical individuals. The behavior of the population as a system cannot be completely understood by mere observation of the behavior of one individual. Returning to multicellular organisms as an example of a cooperative system, a human is more complex than her blood cell. In some situations observing one individual is a misleading way to quantify fitness, but there are also situations (one presented in chapter 2) when observing dense population may be misleading and fitness can only be quantified for an individual in isolation.

Many real populations do not live in a well-mixed environment. While locally, at some small territories, their evolution may be well described by a well-mixed model, single individuals always migrate and colonize new territories. As a result, more distant individuals do not share resources as much and therefore compete less. Since natural selection acts locally, spatial organization might influence selection patterns in some way. On the other hand, some properties may stay universal and independent of the peculiarities of the environmental landscape. This is what I will present in the third chapter of this document.

Chapter 2. Isolated Cell Behavior Drives the Evolution of Antibiotic Resistance

Introduction

Predicting the evolution of antibiotic resistance in bacterial populations is a key challenge (Madigan *et al*, 2009), as the spread of antibiotic resistance has been of increasing concern worldwide(Normark & Normark, 2002). Antibiotics are used in both the clinic and for agriculture, and in addition are produced naturally by many organisms, meaning that antibiotics are present in diverse ecological environments at a wide variety of concentrations(Martínez, 2008). To predict - and possibly prevent - the spread of antibiotic resistance, we must understand the environmental conditions that select for an increase of resistance and what determines the evolutionary fitness of resistant strains.

Antibiotic resistance in microbes is typically quantified by the minimum inhibitory concentration (MIC)(Andrews, 2001) (Wiegand *et al*, 2008)(CLSI document M07-A9, 2012), which is defined as the lowest concentration of antibiotic that will inhibit bacterial growth over a 20 hour period in cultures starting from a standard initial cell density (Clinical & Institute, 2009). The MIC is sometimes used as a proxy for bacterial fitness in the presence of antibiotics (Weinreich *et al*, 2006) (Tan *et al*, 2011) (Lee *et al*, 2010), and in addition is thought to indicate the minimal antibiotic concentration at which there is selection for increased resistance(Yeh *et al*, 2009) (Hermsen *et al*, 2012). Thus, the MIC plays an important role in our understanding of the evolution of antibiotic resistance in bacteria.

However, while the MIC is sometimes considered a single value proxy for fitness, its relationship to evolutionary fitness is often complicated. For β-lactam antibiotics, the oldest and most widely-used class of antibiotics(Bonomo & Tolmasky, 2007), the MIC is frequently subject to the "inoculum effect": its measured value is strongly dependent upon the starting cell density of the culture(Brook, 1989)(Fig. 1). This occurs because resistance to beta-lactams is often achieved viahydrolytic inactivation of the

antibiotic by resistant cells, which can benefit the entire bacterial population by causing overall depletion of antibiotic (Clark *et al*, 2009) (Dugatkin *et al*, 2005). β-lactams are bactericidal and therefore any bacteria that survive the treatment often go through the death phase. The dynamics of these populations can be complex (Yurtsev *et al*, 2013)(Yurtsev *et al*, 2013), and since the MIC is sensitive to the initial cell density, the relevance of a high-density MIC measurement to the evolutionary fitness of individual bacteria is unclear(Goldstein *et al*, 1991).

In this chapter, we demonstrate that the MIC is in many ways a flawed metric for quantifying the fitness of antibiotic-resistant bacteria, due to its dependence upon the cooperative growth dynamics between cells. We find that measuring the direct benefit conferred by resistance for a single, isolated cell is a more robust, meaningful, and useful way to quantify the fitness of a resistant bacterial strain. This single-cell resistance is simply the MIC measured in the limit of low initial cell density, which we call the single-cell MIC (scMIC). This quantity predicts both the direction of selection and the approximate antibiotic concentration at which there is selection for increased resistance. Importantly, these two key predictive properties of the scMIC are independent of the density of the bacterial culture in which selection occurs, and thus the scMIC can provide valuable guidance for researchers and clinicians studying the evolution of antibiotic resistance.

Results

Measurement of single-cell MIC

In this study, we use the β-lactam antibiotic cefotaxime and β-lactam resistant *E. coli* strains(Weinreich *et al*, 2006) to quantify the evolutionary predictive power of the MIC. Each resistant strain expresses a plasmid-encoded TEM β-lactamase enzyme, which can hydrolytically inactivate a wide range of targets(Bush *et al*, 1995) (Jacoby, 2006), including the third-generation cephalosporin cefotaxime(Stemmer, 1994) (Hall, 2002).

Throughout the remainder of this chapter, we use the abbreviation "MIC" to describe the lowest concentration of antibiotic that inhibits growth of a culture over 20 hours; this MIC is a function of the initial cell density. We will denote the specific MIC value for the standard initial cell density (standard density is $5X10^5$ cells/ml) as the MIC*.

Consistent with previous measurements(Brown *et al*, 1981), we observed the inoculum effect in β-lactam resistant *E. coli* TEM strains: the MIC often depends strongly on the initial cell density. In particular, the MIC increases dramatically at high cell densities but plateaus at low initial cell densities. For example, the MIC for *E. coli* expressing β-lactamase TEM-20 varied by three orders of magnitude depending upon the initial cell density. As the cell density decreased, the measured MIC asymptotically approached a limit, which corresponds to the level of resistance of a single, isolated cell: the scMIC (Fig. 1b). Interestingly, this is also the lowest antibiotic concentration that results in cell death at a wide range of cell densities (Fig. S1). Based on these results, we standardized our measurements of the scMIC by using an initial cell density of 500 cells/ml, a thousand times smaller than the standard MIC* initial cell density.

As a metric of the level of antibiotic resistance, the scMIC has several attractive qualities. First, the scMIC can be measured in the same experimental setup as the MIC*, with the only change being a decrease in the initial cell density. Moreover, because the MIC curve plateaus at low cell density, where the scMIC is measured, scMIC measurements are also more robust against experimental errors in the initial cell density. This asymptotic limit also makes it possible to measure scMIC without diluting to the limit of single cells, thus avoiding stochastic effects associated with very small starting cell numbers.

scMIC is the MIC of a single cell.

To demonstrate that the scMIC truly measures the MIC of a single cell (not only in the limit of diluting to single-cell density), we monitored the behavior of a single cell on the agar with various antibiotic concentrations (Fig. 2a). Initially, single cells were scattered at low density on the agar surface. After 2

hours, the cells growing at low antibiotic concentrations formed micro colonies, while those at higher antibiotic concentrations grew as filaments if antibiotic concentration is higher than scMIC. Filament formation has previously been observed in bacteria exposed to antibiotics(Yao *et al*, 2012)(Chung *et al*, 2009); filamentation leads to cell death and the failure to form colonies.

We compared the antibiotic concentration required to prevent colony formation with the scMIC measured in liquid culture. These queantities should be equivalent: each colony observed on an agar plate develops from a single cell that was able to reproduce in a given antibiotic environment. Encouragingly, we find that the single-cell resistance measured on agair is within a factor of two of the scMIC obtained by the liquid dilution method (Fig. 2b), with both quantities being at least an order of magnitude smaller than the MIC*. The fact that very different experimental approaches yield similar quantities gives us confidence that both methods are indeed quantifying the resistance of a single, isolated cell.

While the main method that we use to quantify the scMIC does not involve conventional single cell experimental techniques, we believe that the name "single cell MIC" is accurate for the following reasons. First, experimentally we observe the disappearance of the inoculum effect as the MIC curve plateaus at low cell densities, where dilution prevents significant depletion of the total antibiotic concentration. Second, this liquid dilution method agrees with a true single cell measurement – plating at low density on agar. In this agar plating method every observed colony is a result of growth starting from a single cell, so the presence of a colony is conditioned on the survival of a single cell in a given antibiotic environment. Finally, we used microscopy to directly observe growth of single cells in a variety of antibiotic concentrations and observed qualitatively different behavior below and above the scMIC value.

Selection starts at the scMIC even if cell density is high

Given that the scMIC of a strain is often significantly lower than its MIC*, an important question is what antibiotic concentrations will lead to selection of one strain over another when two strains are in

competition, i.e. which conditions promote the evolution of increased resistance. Antibiotic concentrations below the scMIC of both competing strains are not expected to be strongly selective. A mutant with a higher scMIC value than the background population gains a relative advantage when the antibiotic concentration is at least the scMIC of the background population. At that concentration, the background population will die but the mutant will not. As a result, below the scMIC of the reference strain, the fractional composition of the bacterial population will not change overnight, while if the antibiotic concentration is the environment is above the scMIC of the reference strain, the mutant will rapidly increase in fraction (Fig. 3a,b). Importantly, this prediction should hold true even if the population density is high and the overall MIC of the entire population is therefore higher than the scMIC of either of the two strains.

We tested this prediction experimentally by directly competing what we call the reference strain (TEM-20, scMIC 0.65μg/ml) with its high-scMIC mutant (8μg/ml, mutation E104K). In this experiment, the two strains were labeled with plasmids expressing either yellow or cyan fluorescent proteins, thus allowing us to measure fractions by flow cytometry; labels were swapped in replicates of these experiments (Fig. S2). We found that indeed, selection favoring the E104K mutant begins in the vicinity of the scMIC of the reference strain (Fig. 3b). Note that the cell density is high enough so that the MIC measured at this density is higher than the scMIC of both strains. To demonstrate the generality of our claim that selection starts in the vicinity of the scMIC of the background population, we confirmed that this was also the case for competition between the reference strain and another mutant (A42G mutation , scMIC 1.6μg/ml) (Fig. S3). Selection for a higher-fitness mutant therefore begins when the antibiotic concentration reaches the scMIC of the background population, which is often an order of magnitude lower than the MIC* of the population.

Following the logic in the previous section, the scMIC of a population naturally evolving in the presence of antibiotics should increase over time, as long as the antibiotic concentration is high enough to exert a

selective pressure. The scMIC is also expected to predict the antibiotic concentration where *de novo* mutants with higher scMIC can arise. We performed laboratory evolution experiments at multiple antibiotic concentrations both above and below the scMIC of the starting strain (Fig. 4). In these experiments, we evolved six replicates of our reference-strain *E. coli* at four different cefotaxime concentrations for ~100 generations (daily dilutions by 225X for 13 days, Fig. 4a). As expected from our competition experiments, the cultures that were evolved at antibiotic concentrations lower than the scMIC of the starting populations displayed no increase in the scMIC. In contrast, cultures that were evolved at antibiotic concentrations higher than or equal to the ancestral scMIC displayed a significant increase in resistance measured by the scMIC(Fig. 4b). Note that the effective cell densities at which the populations were evolved are much higher than the density of the scMIC. To confirm the generality of these results, we performed laboratory evolution on two other strains carrying different versions of β-lactamase, and once again found that only the populations evolved at antibiotic concentrations close to or larger than the ancestral scMIC evolved an increase in scMIC (Fig. S4).

In vivo relevance of scMIC

A reasonable concern is that the competition outcome and dynamics between bacterial strains could be qualitatively different during growth inside a host. To explore this, we used the nematode worm *Caenorhabditis elegans*, a widely used model host that can be infected and killed by a variety of human pathogens (Paulander *et al*, 2007)(Moy *et al*, 2006)(Ewbank & Zugasti, 2011). *C. elegans* has been proposed as a model system for tests of antimicrobial efficacy, with improved pharmacokinetics as compared with traditional *in vitro* analysis(Moy *et al*, 2006), and may therefore be useful for assessing the generality of antibiotic treatment-driven dynamics.

Briefly, synchronized adult *C. elegans* were fed on a mixture of 90% reference strain and 10% mutant strain to establish a mixed gut community, and were then incubated in worm media containing varying cefotaxime concentrations (Fig. 5a). After 20 hours of antibiotic treatment, we mechanically disrupted the

worms to release gut-associated bacteria and measured the strain composition of *E. coli* by plating. These experiments were performed at low temperatures (23°C) to prevent heat shock and death of the worms.

Consistent with our *in vitro* competition experiments described above, we found that selection for the more resistant mutant (TEM-52) starts at the scMIC value of the less resistant background allele (Fig. 5b, note that the scMIC of the reference strain, TEM-20, is different in these conditions (Björkman *et al*, 2000)). Our key observation, that selection for increased resistance occurs at the vicinity of the scMIC rather than the MIC*, is therefore valid in both direct liquid culture experiments and in the very different environment of a simple animal host.

Model

We developed a simple model to better understand the inoculum effect and the evolutionary meaning of the scMIC and MIC*. In this model, antibiotic diffuses into the periplasmic space of a bacterial cell to inhibit cell wall synthesis. Resistant bacteria secrete the enzyme into the periplasmic space, where it inactivates the antibiotic(Walsh, 2000) (Fig. 6a). At steady state, the flux of antibiotic into the periplasmic space equals the rate of enzymatic inactivation. The resulting active antibiotic concentration in the periplasmic space is therefore lower than the concentration outside of the cell(Zimmermann & Rosselet, 1977) (Fig. 6b). We assume that the division rate of the cell is a function only of the periplasmic antibiotic concentration, which depends upon both the extracellular antibiotic concentration and the enzyme kinetics. We experimentally found that for our TEM strains in cefotaxime, this growth rate function can be approximated as a step function: cells divide at a normal rate until the antibiotic concentration in the periplasmic space is above some value a_{crit}, at which point cells die at a rate $\sim 2hr^{-1}$ (Fig. 6c,6d, S1,S5).

In this model, the scMIC of a strain is the external concentration of antibiotic that gives rise to a periplasmic concentration of a_{crit}. A nonresistant strain that cannot inactivate antibiotics has a periplasmic

concentration of antibiotic approximately equal to the external concentration, suggesting that a_{crit} is simply the scMIC of a sensitive strain. Therefore,

$$scMIC = a_{crit}\left[1 + \frac{V_{\max}}{C(K_M + a_{crit})}\right],$$

where C is the permeability of the membrane, and V_{max} and K_M are the Michaelis-Menten parameters of the enzyme (the maximum reaction rate of the enzyme and the substrate concentration at which the reaction rate is half of V_{max} respectively). Thus, within this model, a mutant strain with a more efficient enzyme (higher V_{max} and/or lower K_M) will have a higher scMIC. This equation has been proposed to quantify MIC*(Nikaido & Normark, 1987), but it is correct only when the inoculum effect is weak and scMIC is approximately equal to MIC*.

This simple model correctly predicts the relationship of the MIC to the initial cell density for reference strain and the mutant (Fig. 6e). For both strains, there are two free parameters that describe the efficiency of the particular version of the enzyme in hydrolyzing cefotaxime: the Michaelis-Menten parameters V_{max} and K_M. Our model also provides insight into the upper bound for the cell density that should be used in the definition of scMIC. For the strains that we use, the density should be less than 10^4 cells per ml (see Chapter 3 for the reasoning), which our proposed definition of scMIC indeed satisfies.

Our model agrees with the experimental finding that independent of initial cell density, selection favoring the competitor with the higher scMIC will begin when the antibiotic concentration approaches the scMIC of the less resistant strain (Fig. 6f). In our experiments, selection starts at even somewhat lower antibiotic concentrations than predicted by our model (Fig. 3b), likely because this minimalist model assumes that the antibiotic has no effect until the cell begins to die (see Fig. 6d); a gradual decrease in the growth rate with antibiotic concentration would result in selection at concentrations below the scMIC. In either case,

selection may occur at antibiotic concentrations that are orders of magnitude lower than the MIC*.

Our model also predicts that the strength of selection for increased scMIC will depend non-monotonically on the antibiotic concentration, leading to the counter-intuitive effect whereby adding additional antibiotic decreases the ability of a mutant with higher scMIC to spread against the background population (Fig. 6f). This surprising prediction was also validated in both our in vitro and in vivo experiments (Fig. 3; Fig. 4). The strength of selection decreases above the scMIC of the winning strain because the released enzyme from the dying bacteria(Sykes & Matthew, 1976) hydrolyses antibiotic faster than the rate of antibiotic hydrolysis within a cell. This effect can be understood within a framework of altruistic death, either deterministic(Tanouchi *et al*, 2012) or stochastic(Ackermann *et al*, 2008), in which the death is favorable for the population if the benefit from the released public goods is strong enough.

Finally, the model also successfully predicts that lower initial cell densities will experience stronger selection (Fig. 6f,S6). This is because lower initial cell densities will take longer to inactivate the antibiotic, thus extending the window for selection during which the less-resistant strain experiences cell death. On the contrary, the antibiotic concentration at which selection starts does not depend strongly on the cell density. This makes sense since the periplasmic antibiotic concentration at the beginning of the experiment is independent of the cell density. The cell density does, however, alter the temporal dynamics of the antibiotic concentration over the course of the day, thus modifying the strength of selection favoring the strain with higher scMIC. Although this simple model works well at low to moderate antibiotic concentrations, it does not explain the behavior of the inoculum effect and selection curves at high antibiotic concentrations. To account for both discrepancies, we can allow for degradation of the β-lactamase enzyme in the model (Fig. S7).

MIC*-scMIC relationship

In this system, cooperative resistance and the inoculum effect occur due to enzymatic inactivation of antibiotics. The population's collective capacity to inactivate the antibiotic is expected to increase with both cell density and the efficiency of the resistant enzyme. We therefore hypothesized that strains carrying a highly efficient enzyme (and therefore showing high scMIC) would also have a large difference between the scMIC and the high-density MIC*.

To characterize this relationship, we measured the MIC* and scMIC in cefotaxime for 16 *E. coli* strains with different versions of the TEM β-lactamase enzyme (Fig. 7a) (Weinreich *et al*, 2006). We found that the inoculum effect is strong for all the highly resistant strains, with the MIC* often being two orders of magnitude higher than the scMIC. However, at low levels of resistance, the MIC* and scMIC values are nearly the same. Our model is able to explain this relationship between the MIC* and the scMIC by assuming that all of the strains are equivalent except for variation in the V_{max} of the β-lactamase enzyme (though *in vitro* measurements indicate that both V_{max} and K_M are sensitive to mutations in the enzyme(Philippon *et al*, 1989) (Wang *et al*, 2002)).

Although in general the MIC* increases together with the scMIC, we found some exceptions (Fig. 7a). For example, the A42G mutant of TEM-20 has an MIC* that is almost four times larger than that of TEM-15 (64 μg/ml vs 18 μg/ml; pair drawn in black in Fig. 7a). Nevertheless, our measured scMIC for TEM-15 is if anything somewhat higher (1.59 μg/ml with 68% confidence interval (1.41; 1.78) vs 1.78 μg/ml with 68% confidence interval (1.59; 2)). The MIC* and scMIC can have different orderings because the MIC* reflects the cooperative hydrolysis of the antibiotic at high cell density (and often scales with V_{max} of the enzyme) whereas scMIC reflects the "selfish" hydrolysis in the periplasmic space (and scales as the ratio of V_{max}/K_M for large enough K_M). We expect this distinction to be relevant for any resistance mechanism governed by enzymatic inactivation of a drug. Enzymatic inactivation has been an observed mechanism of resistance against several classes of antibiotics, including β-lactams,

aminoglycosides(Shaw *et al*, 1993) and macrolides(Leclercq, 2002), suggesting that these ideas may have broad relevance in the study of antibiotic resistance.

Given that both the MIC* and the scMIC are intended to measure the level of resistance, this prompts the question: which strain is favored in the presence of the antibiotic? More generally, does selection favor an increase in MIC*, as is generally assumed, or does selection instead favor an increase in scMIC as we argue here? We competed the two strains and found that the antibiotic selects for TEM-15 (Fig. 7b), suggesting that selection does indeed maximize the scMIC rather than the MIC*. To confirm that this conclusion is not specific to this particular pair of strains, we repeated the competition experiments with another pair exhibiting a reversal between scMIC and MIC* and obtained similar results (Fig. S8). Finally, we analyzed the evolved lines in Fig. 1c and found several cases in which laboratory evolution led to an increase in scMIC but no discernible increase in the MIC* (Fig. S9); a decrease in MIC* has also been observed in laboratory fungal evolution(Cowen *et al*, 2001)). Taken together, these results argue strongly that selection acts on the scMIC rather than the MIC*, since the scMIC is the quantity that directly measures the fitness of an individual cell.

Discussion

Understanding the role of collective resistance in bacterial antibiotic response is essential in predicting the evolution of antibiotic resistance. When mutants arise in an antibiotic-resistant population, the MIC* is often thought to indicate both the direction of selection and the antibiotic concentration that will lead to strong selection for increased resistance. We have found here that the MIC* can fail in both of these tasks, and found instead that the scMIC—the resistance of a single, isolated cell—accurately predicts the evolutionary behavior of bacterial populations exposed to an antibiotic.

While the scMIC is a better way of predicting evolution than the MIC*, the MIC* still contains important information that could be used for purposes other than predicting evolution. For instance, the MIC* captures the population-level resistance due to effects such as the collective inactivation of a drug. This population-level resistance is useful for determining proper antibiotic dosage and regimen because the entire population of many cells needs to be killed, and therefore the cooperative part of resistance cannot be ignored. It is important to stress that predicting evolution and estimating the antibiotic concentration required to kill a population of a given size are very different questions; while the former requires understanding the costs and benefits to a single cell, the latter requires quantification of the population-level resistance.

Although our experiments have focused on the β-lactam cefotaxime, we expect that similar phenomena may be observed for other drugs that show an inoculum effect. The inoculum effect can often be caused by enzymatic degradation of antibiotics, and plasmid-borne antibiotic-degrading enzymes are widespread among bacteria in natural environments (Bennett, 2008). Even when enzymatic inactivation does not occur, the inoculum effect can be generated by antibiotic titration, as has been observed for ribosome-inhibiting antibiotics(Tan *et al*, 2012). The distinction between the scMIC and the MIC* may therefore be relevant across many classes of antibiotics.

Other work has suggested that the MIC* may not perform well as a measure of evolutionary fitness, even where resistance is not density-dependent. For example, a recent study demonstrated that sub-MIC* levels of tetracycline, aminoglycosides, and fluoroquinolone antibiotics can select for cells carrying an antibiotic resistance plasmid(Gullberg *et al*, 2011). The resistance mechanism in this previous study was not cooperative, and inoculum effects were not observed; selection occurred when growth inhibition of sensitive strains at sub-MIC* antibiotic concentrations was greater than the growth disadvantage associated with resistance gene expression, a point designated by authors as the minimal selective concentration (MSC). Though different mechanisms were implicated in this previous work and in the

present study, in both cases selection occurred when single-cell growth of the less-resistant strain was suppressed at sub-MIC* drug concentrations. We conclude that even in absence of cooperative resistance, the MIC* is unlikely to be a reliable measure of evolutionary fitness at low drug concentrations.

In this chapter and in the discussion above, we have assumed that the growth rate falls as a step-function with increasing antibiotic concentrations, which is a reasonable approximation for most beta-lactams and for a variety of other antibiotics(Wiuff *et al*, 2005) (Johnson & Levin, 2013). However, for some antibiotics (such as tetracycline), the growth rate falls gradually with increasing antibiotic concentrations. In particular, very low concentrations of antibiotic have a modest but potentially significant effect on bacterial growth. In this situation, it is possible to get selection for antibiotic resistance at sub-MIC concentrations of antibiotic, even in the absence of collective inactivation of the antibiotic (in which case the scMIC is equal to the traditional MIC)..Collective antibiotic degradation is therefore not the only mechanism for sub-MIC selection for antibiotic resistance.

It is important to recognize that antibiotic degradation need not produce a strong inoculum effect. When enzymatic degradation is slow, modeling and experimental results indicate that the scMIC and MIC* will be small and their values will be similar (Fig. 7a). In this case, we still expect selection to be non-monotonic with antibiotic concentration as observed here, where strongest selection for a high-resistant occurs at drug concentrations that inhibit the background strain but allow the mutant to grow (Fig. 3c, S6, S8). In fact, non-monotonic strength of selection has been observed as a function of cefotaxime concentration in E. coli expressing weak alleles of TEM β-lactamase (Negri *et al*, 2000) with no distinction between scMIC and MIC*.

Unlike the MIC*, the scMIC can in principle be measured in a shorter time frame than 20 hours. The time it takes to determine the resistance level of bacteria is crucial for patient survival(Soong & Soni, 2012) and several methods have been suggested to quantify the level of resistance within a few hours using

microfluidics (Rapid antibiotic susceptibility testing by tracking single cell growth in a microfluidic agarose channel system - Lab on a Chip (RSC Publishing))(Mohan *et al*, 2013). Since these methods can determine the antibiotic concentration when the growth of a single cell is significantly inhibited, they can be used for scMIC determination. They cannot however be used for MIC* determination since the experiments do not probe whether a larger population of cells would have survived the antibiotic treatment after a longer period of exposure. As we demonstrated here (Fig. 2b), it is possible to measure scMIC without using microfluidic devices by simply plating cells on agar with various antibiotic concentrations. Although in the experiments described here we waited for the cells to grow into visible colonies, in principle microscopy imaging could be done a few hours after plating as a rapid diagnostic to determine whether a bacterial strain can grow in high antibiotic concentrations (ie resistant)(Chadwick, 1966) .

The resistance of the entire population – the MIC* - incorporates the cooperative nature of bacterial growth, and generally differs from the resistance of a single cell, quantified by the scMIC. Put most simply, selection acts on individuals and favors genotypes that perform better as individuals, and as such the single cell minimum inhibitory concentration is the proper metric for predicting which mutations will be favored by selection.

Materials and Methods

Strains

TEM strains were obtained from Daniel Weinreich(Weinreich *et al*, 2006). All strains were *E. coli* DH5α transformed with pBR322 plasmids carrying different alleles of TEM-1. These alleles represented all

possible combinations of presence or absence of A42G, E104K, M182T and G238S mutations in the β-lactamase gene.

MIC/scMIC

For MIC/scMIC measurements, the strains were cultured at 37C in 5mL LB with 50 μg/ml piperacillin (for plasmid selection) for 18-20 hours with 300 rpm shaking in 50 ml falcon tubes. Cultures were then diluted to the initial optical densities and grown in serial dilutions of cefotaxime in 96-well plates at 37C for 20 hours with 500 rpm shaking. MIC was determined by the lowest concentration that prevented bacterial growth (OD<0.3). All measurements were done in triplets.

Competition experiments.

For competition experiments, we transformed TEM strains with plasmids constitutively expressing either CFP or YFP (plasmids pZS25O1+11-Cerluean and pZS25O1+11-YFP). Two cultures of different colors were grown from single colonies for 18-20 hours in 50 μg/ml of piperacillin and 50 μg/ml of kanamycin for plasmid selection. These cultures were then mixed and grown for another 20-22 hours in 50 μg/ml of piperacillin and 50 μg/ml of kanamycin to synchronize the growth phases of the two strains. The purpose of synchronization was to eliminate any experimental variability and experimental effects due to the difference in the growth phases of the two cultures in the beginning of the experiment (in particular, synchronization of the lag time is important for reproducibility).The synchronized mixed culture was diluted to multiple initial cell densities and exposed to various cefotaxime concentrations on 96-well plates. After 25 hours of the experiment, the cultures were diluted in PBS 1:900 and measured at the flow cytometer. For the competition of TEM-15 and A42G mutant of TEM-20, the second day of growth of the two strains together before the addition of cefotaxime was done with no piperacillin present. The reason for that is that piperacillin scMIC of TEM-15 is smaller than 50 μg/ml and the prepared initial fraction shifted significantly over the course of 20-22 hours growth. We confirmed that it did not happen to our other strains that we used for other competition experiments.

Competition experiments in a *C. elegans* model

Synchronized cultures of adult *C. elegans* were produced according to standard protocols (Stiernagle, 2006). Unless otherwise specified, all experiments were performed at 23°C; liquid culture experiments were performed with shaking at 300 RPM. Asynchronous cultures of the temperature-sensitive sterile mutant *C. elegans* AU37 were grown at permissive temperatures (16C) on NGM agar plates with *E. coli* OP50 as a food source; recently starved plates were washed to retrieve adults for bleach/NaOH synchronization. Eggs were incubated 24 hours at 23°C in M9 worm buffer with shaking at 300 RPM, and L1 larvae were transferred to NGM + OP50 plates at 23°C to produce sterile adults. Young adult worms were washed from agar plates and incubated 24 hours in liquid S medium with heat-killed OP50 as a food source and 100 μg/mL kanamycin to remove any adhered or internalized OP50, producing microbe-free 2-day adults for colonization.

Bacteria were grown as described for *in vitro* competition experiments, resuspended to uniform densities (~10^9 cells/mL) in liquid S medium, and mixed to obtain feeder cultures containing 90% TEM-20 and 10% TEM-52. Synchronized adult worms were colonized by feeding for 36 hours in 1 mL bacterial cultures in 24-well plates, which were covered with BreatheEasy transparent membranes (Diversified Biotech) to allow gas exchange and loosely covered with foil to protect cultures from light. After colonization, worms were washed to remove external bacteria, then transferred to fresh 24-well plates in 1 mL liquid cultures of S medium containing heat-killed OP50 as a food source and different concentrations of cefotaxime (0-0.8 μg/mL) for competition. After 20 hours incubation with cefotaxime, worms were washed and mechanically disrupted by grinding in 25 μL M9 worm buffer + 0.1% Triton X-100 using a Kimble Kontes motorized pestle. The resulting bacterial suspension was diluted in M9 worm buffer and plated on LB agar. Colony forming units per worm were determined for each bacterial strain by counting YFP and CFP colonies after 48 hours.

Evolution

For evolution experiments, we started with TEM-19, TEM-20 and the A42G mutant of TEM-17. All strains were exposed to 4 antibiotic concentrations, and for each antibiotic condition 6 independent populations were evolved. Every day, we diluted 1:225 the evolving cultures to new media with fresh antibiotic. After 13 days, scMICs of all cultures were measured and the β-lactamase genes were sequenced.

Figures to Chapter 2.

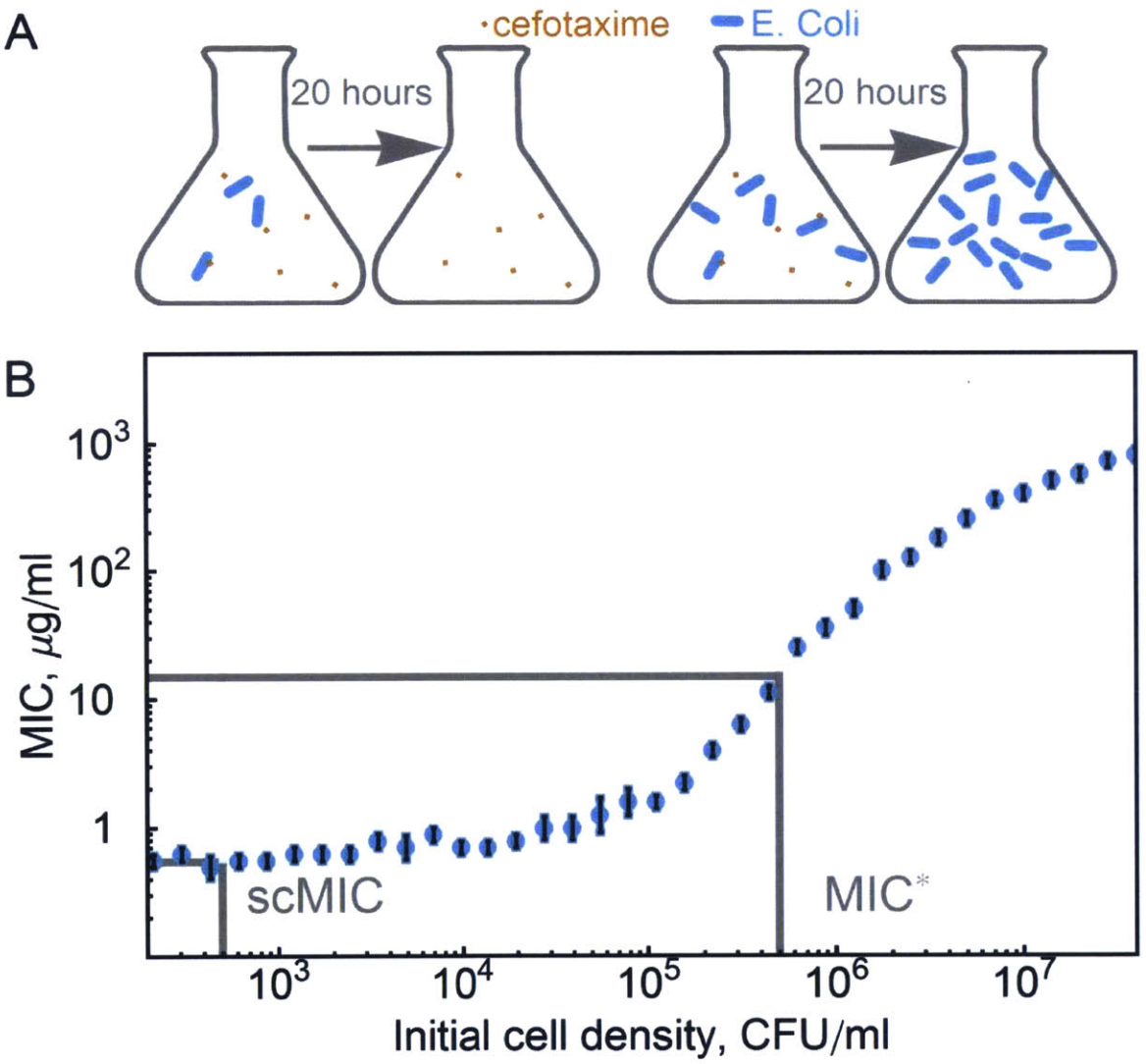

Figure 1: MIC levels off in the limit of small densities, asymptotically approaching scMIC.

(a) Design of the inoculum effect experiment. Initial cell density determines whether in 20 hours the population survives at a given antibiotic concentration. On the left, the cell density is not enough to produce necessary amount of enzyme that breaks antibiotic. Therefore, in 20 hours all cells are dead. On the right, the cell density is high enough to produce enough enzymes, and therefore in 20 hours the population survives the treatment and no antibiotic is left in the media.

(b) We define the scMIC as the measured minimum inhibitory concentration (MIC) at low starting cell densities. The measured MIC of TEM-20 varies by three orders of magnitude depending upon the starting cell density and asymptotically approaches a limit at low cell densities. The gray bars correspond to the initial cell densities for MIC* and scMIC. The error bars are the maximum of a discretization error and the standard error of the mean of three measurements.

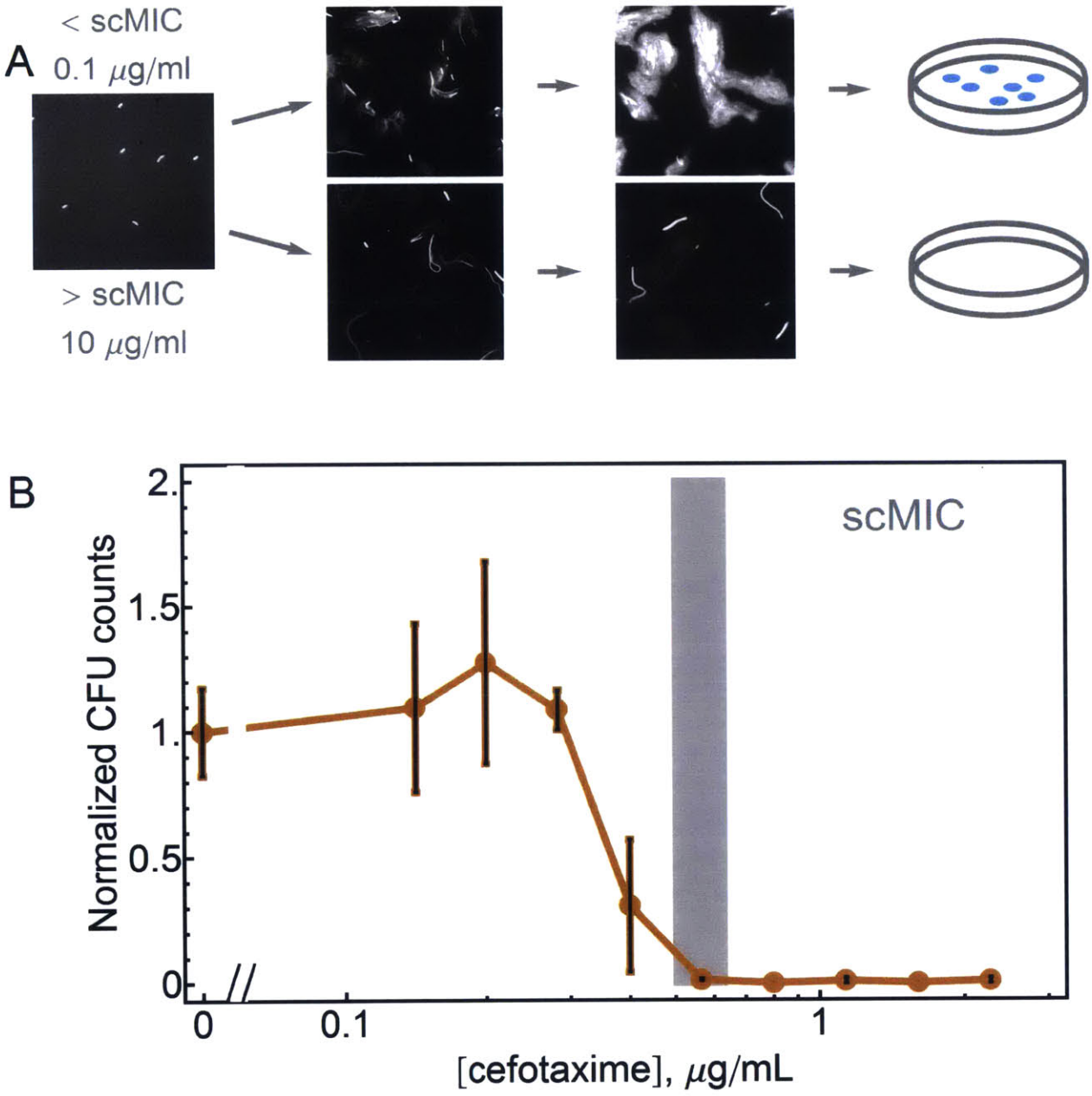

Figure 2: scMIC is the MIC of a single cell.

(a) The diagram of the time evolution of cell density on the surface of the agar media at two antibiotic concentrations: below (the top row of images) and above (the bottom row of images) the scMIC of the imaged strain. We initially pipette diluted saturated culture on the surface of the agar (0.4%) and take an image on which we can see distinct single cells scattered on the surface. While at antibiotic concentration

below the scMIC an exponential growth of cells is happening during first 5 hours, at the antibiotic concentration above the scMIC cells undergo filamentation process and do not form colonies in 1 day.

(b) The scMIC can also be estimated by plating cells on agar. Saturated cultures of TEM-20 were evenly spread on agar plates with various cefotaxime concentrations. The colony forming units (CFU) were evaluated for 2 independent cultures and normalized by the CFU obtained without antibiotics. The error bars are the maximum of the two Poissonian errors for 0 antibiotic concentration and the standard error of the mean for all non-0 antibiotic points.

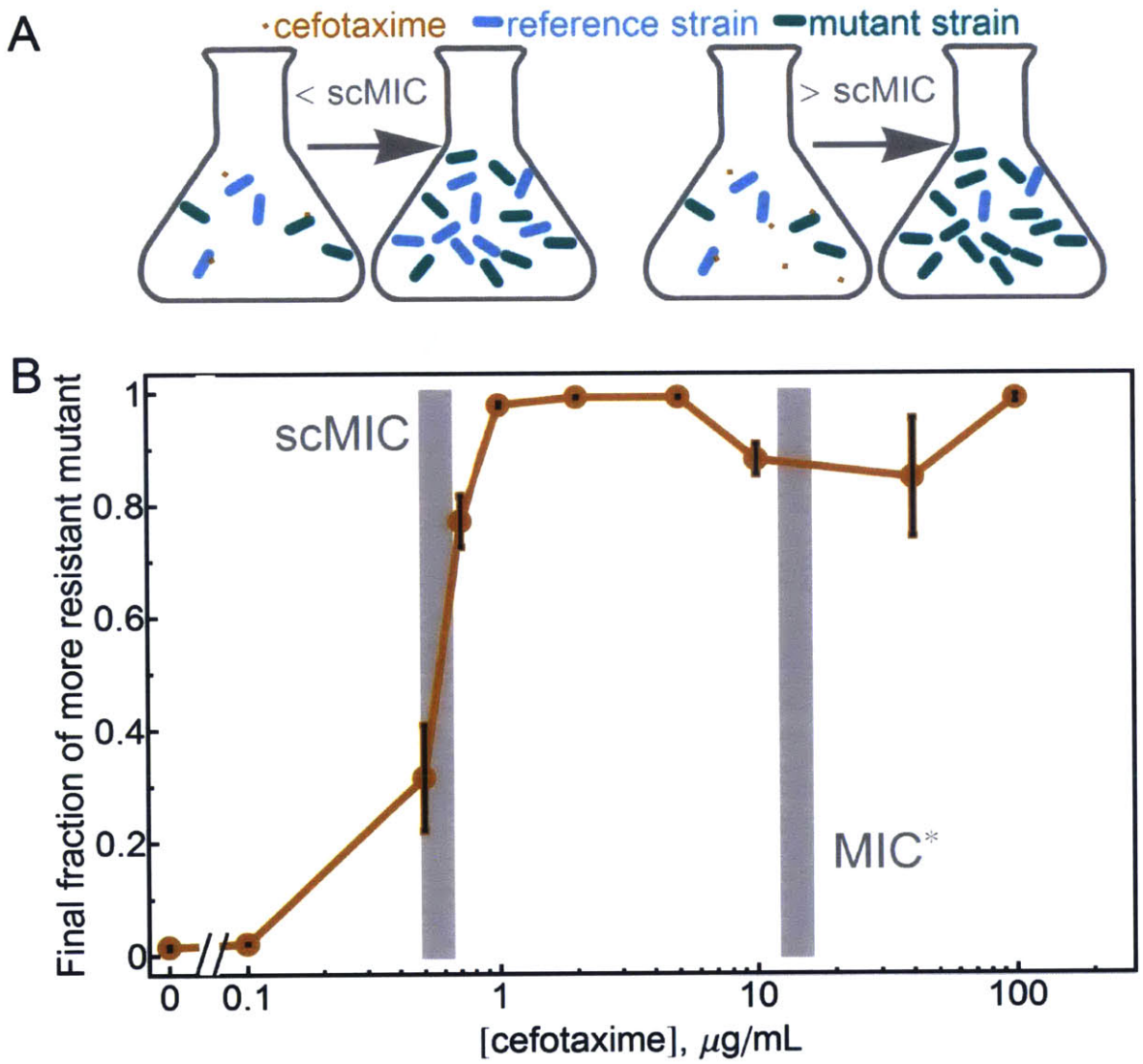

Figure 3: Selection starts at the scMIC even if the cell density is high.

(a) Design of the competition experiment. The mixture or reference and mutant strain of a certain (high enough) density grow overnight in environment with different antibiotic concentrations. When the initial antibiotic concentration is below the scMIC of the reference strain, the mutant strain does not have selective advantage and its fraction remains unchanged after overnight incubation. When the initial antibiotic concentration is above scMIC of the reference strain, the mutant strain has higher fitness and its fraction in the population increases after overnight incubation.

(b) In competition of the reference and mutant strain, selection for the more resistant mutant begins at antibiotic concentrations near the scMIC, not the MIC*, of the reference strain. For most of the data points, the mean values for 9 or 10 different cultures are presented. The pairs of two types of strain coloring are presented: in some of the samples, reference strain had YFP label and mutant strain had CFP label, and in some other samples reference strain had CFP label and mutant strain had YFP label. No difference in final fraction of the mutant between these two types of labeling was observed. For the highest cefotaxime concentration, the average of 3 data points is shown. The error bars are the standard error of the mean. The gray bars correspond to the MIC* and scMIC values of the reference strain.

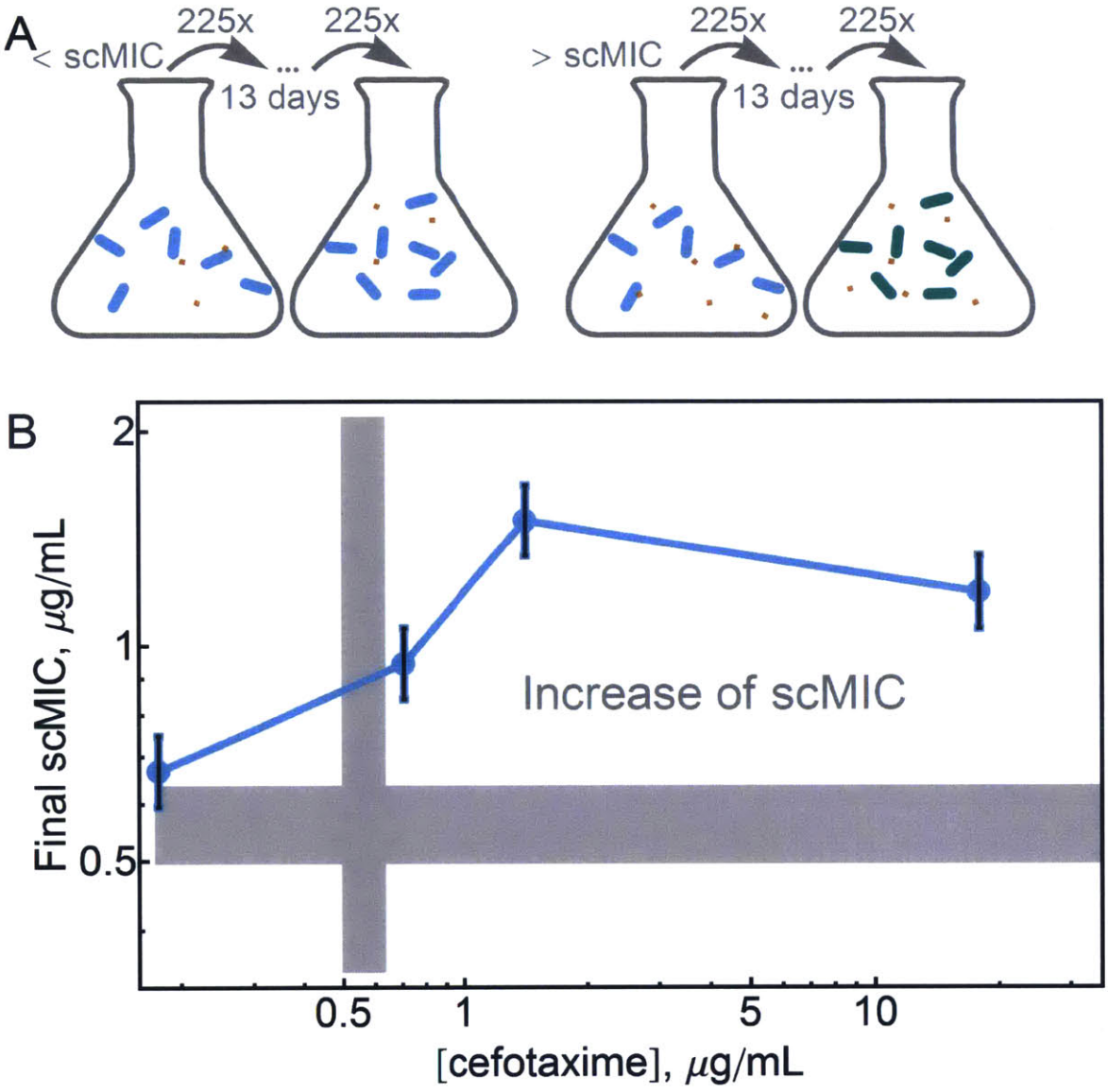

Figure 4: Higher levels of resistance evolve at antibiotic concentrations above scMIC.

(a) Design of the laboratory evolution experiment. Identical clonal populations of cells are evolved over 13 days with daily dilution scheme in environments with various antibiotic concentrations. The increase of the scMIC of the population at the end of the experiment is observed in the environments where antibiotic concentrations are above scMIC of the initial population.

(b) Laboratory evolution experiments of TEM-20 confirm that increase of resistance evolves in antibiotic concentrations equal to and larger than the scMIC. Plotted is the scMIC measured after 13 days versus the concentration of cefotaxime the strains were evolved at. The error bars are the standard errors of the mean of six independent evolved populations. The gray bars correspond to the initial scMIC values.

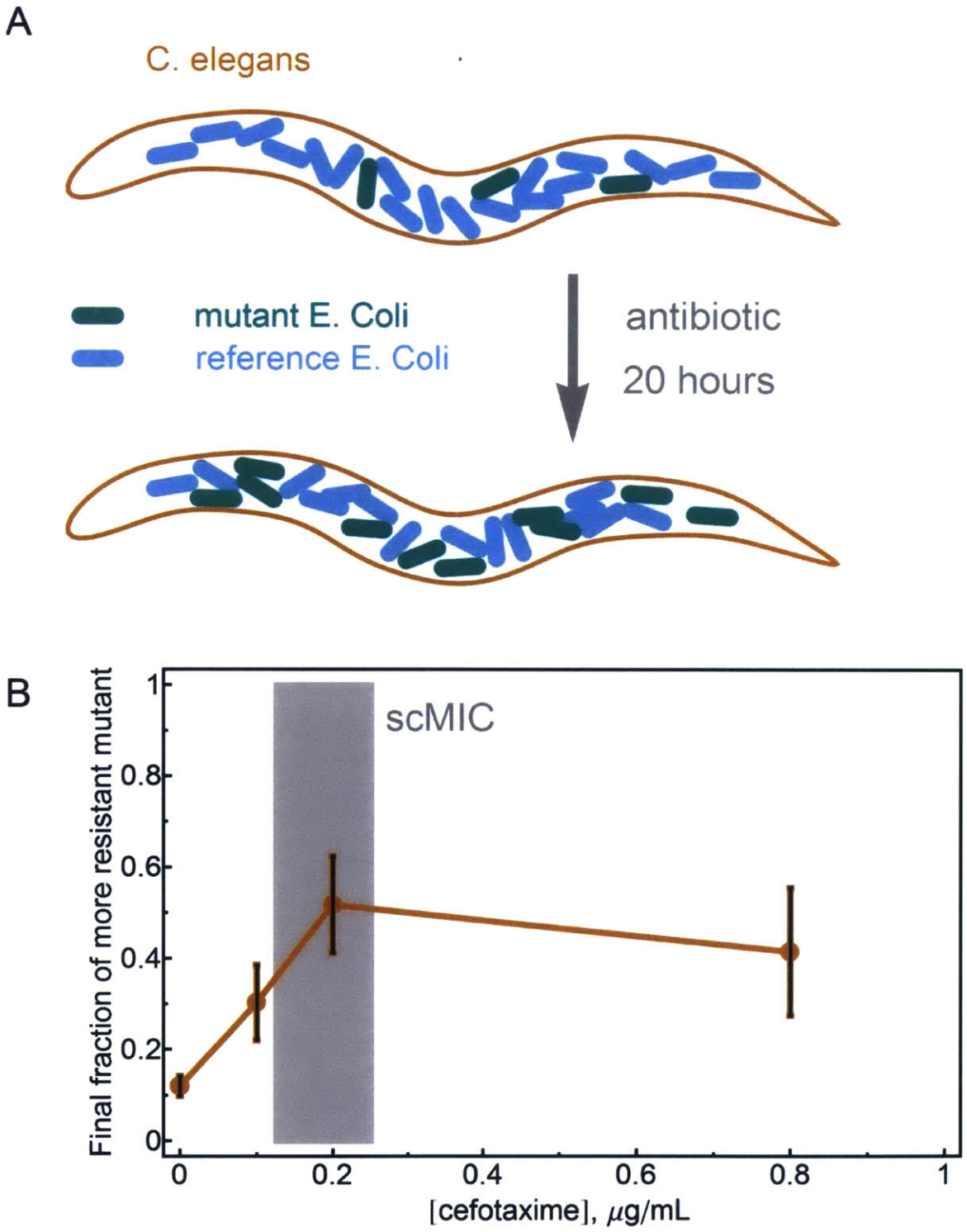

Figure 5: In complex environments, scMIC is predicting selection.

(a) Schematic representation of the in vivo experiment. *C. elegans* were colonized with a mixture of TEM-20 (90%) and TEM-52 (10%) and were grown treated with antibiotic for 20 hours before the final fraction of TEM-52 was measured.

(b) Selection for increased resistance begins at antibiotic concentrations near the scMIC, as in the in vitro measurements. The error bars are the standard error of the mean of 3 measurements. The discrepancy between the in vivo scMIC and the in vitro measurements is likely due to differences in respective environmental conditions, such as nutrient availability and temperature.

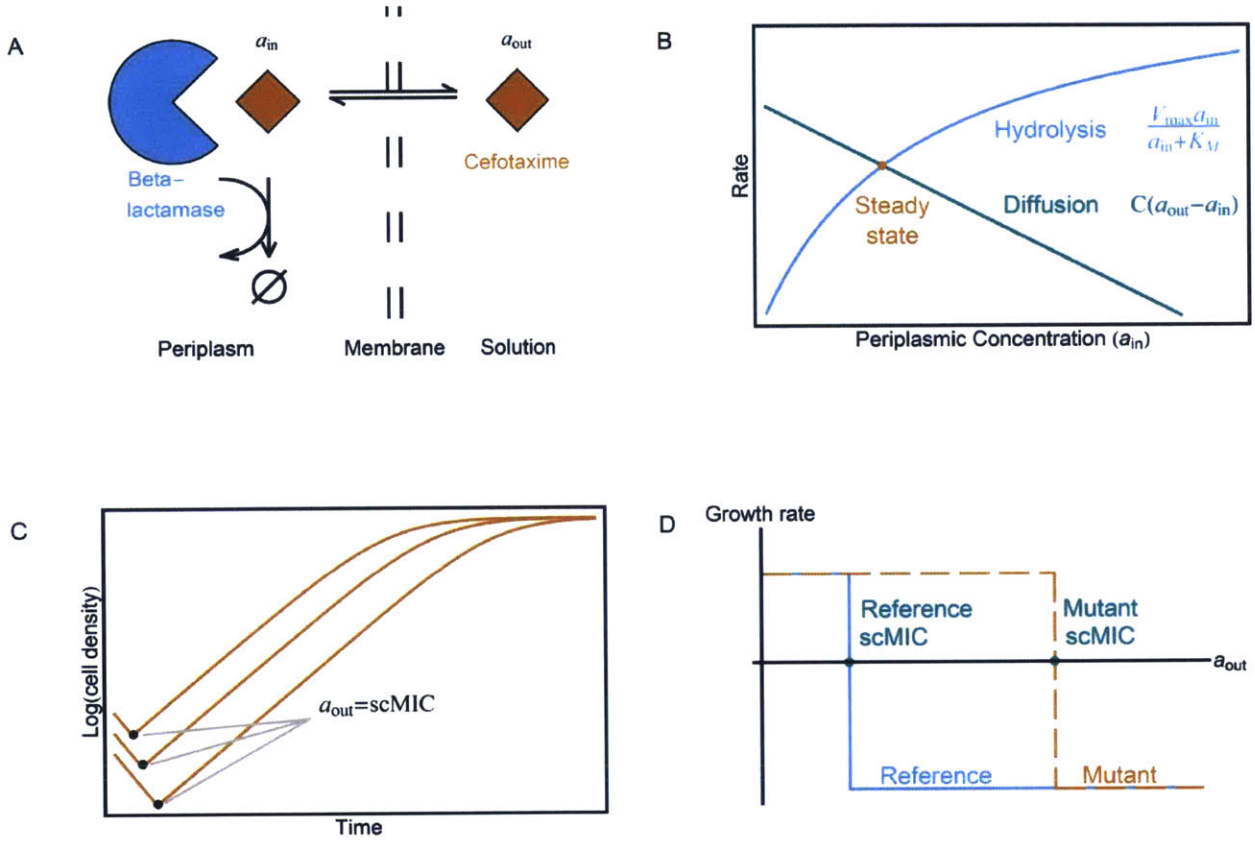

Figure 6: A simple model captures predictive power of the scMIC.

(a) Cefotaxime diffuses into the periplasmic space of the cell, where the enzyme β-lactamase hydrolyzes cefotaxime. a_{in} and a_{out} correspond to the cefotaxime concentrations in the periplasmic space and outside of the cell, respectively.

(b) At steady state, the diffusion rate of cefotaxime into the cell equals the Michaelis-Menten hydrolysis rate of cefotaxime within the cell. The corresponding cefotaxime concentration inside the periplasmic space is therefore smaller than the concentration outside the cell. C is a permeability parameter; V_{max} and K_m characterize the hydrolytic activity of the enzyme.

(c) Bacterial growth curves with the same initial antibiotic concentrations but different starting densities. The cells die until the external concentration of cefotaxime reaches the scMIC of the strain.

(d) The growth/death rate is a step function of the external cefotaxime concentration, as this determines the periplasmic concentration. Strains with different versions of TEM enzyme will have different scMIC values, which is the external antibiotic concentration at which the growth rate becomes negative (death).

(e) The fits of the inoculum effect curves of the reference and mutant strains (dark regions correspond to the fitting interval). The error bars are the maximum of a discretization error and the standard error of the mean of three measurements.

(f) The model prediction for competition experiments, with a 1% initial fraction of the mutant. At the scMIC of the reference strain, the final fraction of the mutant strain starts to increase, indicating that selection for the more resistant mutant starts near the scMIC. Different colors correspond to different initial cell densities (labeled in CFU/ml). The error bars are the standard error of the mean ($n = 9 - 10$ for most data points). The gray bar corresponds to the scMIC of reference strain. For the model, parameter values are provided Chapter 3.

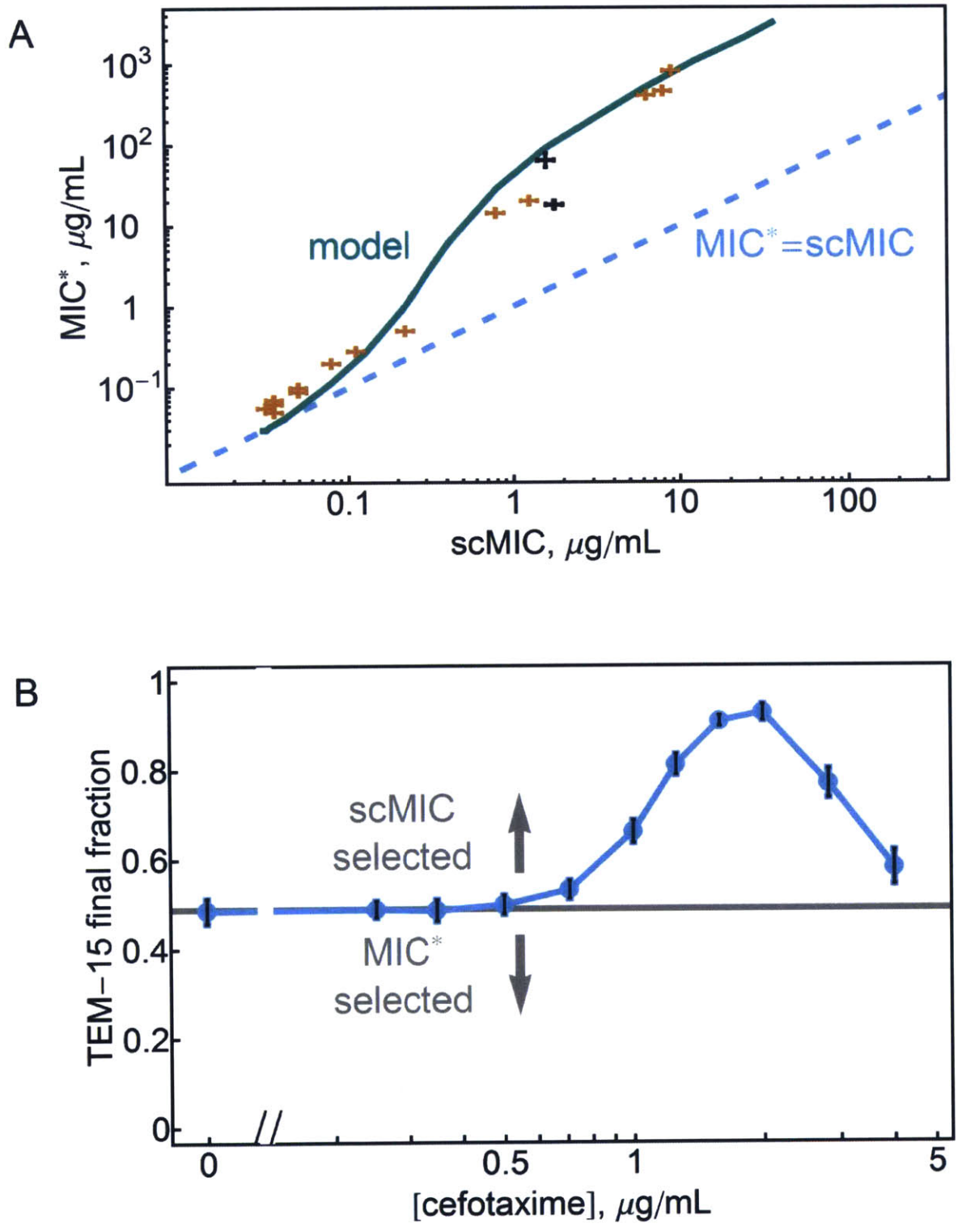

Figure 7: While scMIC-MIC relation can be complex, the scMIC always determines the direction of

selection.

(a) MIC* and scMIC typically increase together. Our model accurately predicts the general relationship between MIC* and scMIC. Plotted is the MIC* and scMIC values for 16 different TEM mutants. Varying only V_{max} in our model (teal) explains the experimental trend (K_M=10 μg/ml). MIC*=scMIC line (dashed blue) shows that MIC* and scMIC are similar for strains with low resistance, whereas MIC* is more than two orders of magnitude larger than scMIC for strains with high resistance. TEM-15 and the A42G mutant of TEM-20 are black. Error bars are the maximum of the standard error of the mean of three measurements and a discretization error associated with the microdilution method (Chapter 3).

(b) Selection favors an increase of scMIC not MIC*. The competition experiment of TEM-15 and the A42G mutant of TEM-20 (initial fraction plotted as horizontal line, initial cell density 5x10^5 cells/ml). TEM-15 has a somewhat higher scMIC (1.78 μg/ml vs 1.59 μg/ml), while the A42G mutant of TEM-20 has a much higher MIC* (64μg/ml vs 18 μg/ml). For cefotaxime concentrations above the scMIC of the A42G mutant of TEM-20, the TEM-15 strain is selected for, indicating that selection maximizes the scMIC rather than the MIC*. Error bars are the standard errors of the mean of 4 independent populations.

Chapter 3. Supplemental Information for Isolated cell behavior drives the evolution of antibiotic resistance

1 Model

1.1 Model description

To model the growth of a single strain, we used the following system of equations.

$$\frac{\mathrm{d}a_{out}(t)}{\mathrm{d}t} = -Cn(t)(a_{out}(t) - a_{in}(t)) - y(t)\frac{V_{max}a_{out}(t)}{a_{out}(t) + K_M}$$

$$\frac{\mathrm{d}n(t)}{\mathrm{d}t} = \begin{cases} \gamma n(t)\left(1 - \frac{n(t)}{n_{max}}\right), & a_{in} < scMIC_{Dh5\alpha} \\ -\gamma_d n(t), & a_{in} \geq scMIC_{Dh5\alpha} \end{cases}$$

$$\frac{\mathrm{d}y(t)}{\mathrm{d}t} = \begin{cases} 0, & a_{in} < scMIC_{Dh5\alpha} \\ -\frac{dn(t)}{dt}, & a_{in} \geq scMIC_{Dh5\alpha} \end{cases} \quad (1)$$

$$C(a_{out}(t) - a_{in}(t)) = \frac{V_{max}a_{in}(t)}{a_{in}(t) + K_M}$$

Where

$a_{out}(t)$ - antibiotic concentration in the well (outside the cell);

$a_{in}(t)$ - antibiotic concentration inside the cell;

$n(t)$ - cell density (OD);

$y(t)$ - cell density of dead (lysed) cells (OD);

C - diffusion parameter;

V_{max}, K_M - Michaelis-Menten parameters for beta-lactamase;

γ- growth rate;

γ_d - death rate;

$scMIC_{Dh5\alpha}$ - scMIC of Dh5a;

n_{max} - saturation OD.

The first equation describes two mechanisms by which the antibiotic concentration $a_{out}(t)$ in the well decreases: antibiotic can diffuse inside a cell or can be degraded by the beta-lactamase in the media released by the dead lysed cells. The second equation describes the dynamics of cell density $n(t)$ as a function of the antibiotic concentration inside the cell (in the periplasmic space): the cells grow logistically when the concentration in the periplasm is lower some value and die and lyse exponentially when the antibiotic concentration exceeds this value. The third equation describes the time evolution of the density of the dead and lysed cells $y(t)$: whenever antibiotic concentration exceeds the scMIC of DH5a, any change in a cell density $n(t)$ is due to the cell death, therefore the density of lysed cells $y(t)$ increases by the same amount as by which the cell density $n(t)$ decreases; there is no change in the density of lysed cells $y(t)$ when periplasmic concentration of antibiotic $a_{in}(t)$is low enough for cells to divide. The last equation describes the balance between the influx of antibiotic from the environment to periplasm of the cell and enzymatic inactivation of antibiotic in the periplasm(Zimmermann & Rosselet, 1977).

The OD units for cell density correspond to OD600 - absorbance or optical density at 600 nm wave length light of 1 cm-wide sample of the cell culture. The OD of 1 corresponds to $4 \cdot 10^8$ CFU per ml.

For competition experiments, we use the following system of equations:

$$\frac{\mathrm{d}a_{out}(t)}{\mathrm{d}t} = -Cn^{(1)}(t)(a_{out}(t) - a_{in}^{(1)}(t)) - y^{(1)}(t)\frac{V_{max}^{(1)}a_{out}(t)}{a_{out}(t) + K_M^{(1)}} - Cn^{(2)}(t)(a_{out}(t) - a_{in}^{(2)}(t))$$

$$- y^{(2)}(t)\frac{V_{max}^{(2)}a_{out}(t)}{a_{out}(t) + K_M^{(2)}}$$

$$\frac{\mathrm{d}n^{(1)}(t)}{\mathrm{d}t} = \begin{cases} \gamma n^{(1)}(t)\left(1 - \dfrac{n^{(1)}(t) + n^{(2)}(t)}{n_{max}}\right), & a_{in}^{(1)} < scMIC_{Dh5\alpha} \\ -\gamma_d n^{(1)}(t), & a_{in}^{(1)} \geq scMIC_{Dh5\alpha} \end{cases}$$

$$\frac{\mathrm{d}n^{(2)}(t)}{\mathrm{d}t} = \begin{cases} \gamma n^{(2)}(t)\left(1 - \dfrac{n^{(1)}(t) + n^{(2)}(t)}{n_{max}}\right), & a_{in}^{(2)} < scMIC_{Dh5\alpha} \\ -\gamma_d n^{(2)}(t), & a_{in}^{(2)} \geq scMIC_{Dh5\alpha} \end{cases}$$

$$\frac{\mathrm{d}y^{(1)}(t)}{\mathrm{d}t} = \begin{cases} 0, & a_{in}^{(1)} < scMIC_{Dh5\alpha} \\ -\dfrac{dn^{(1)}(t)}{dt}, & a_{in}^{(1)} \geq scMIC_{Dh5\alpha} \end{cases}$$

$$\frac{\mathrm{d}y^{(2)}(t)}{\mathrm{d}t} = \begin{cases} 0, & a_{in}^{(2)} < scMIC_{Dh5\alpha} \\ -\dfrac{dn^{(2)}(t)}{dt}, & a_{in}^{(2)} \geq scMIC_{Dh5\alpha} \end{cases} \quad (2)$$

$$C(a_{out}(t) - a_{in}^{(1)}(t)) = \frac{V_{max}^{(1)}a_{in}^{(1)}(t)}{a_{in}^{(1)}(t) + K_M^{(1)}}$$

$$C(a_{out}(t) - a_{in}^{(2)}(t)) = \frac{V_{max}^{(2)}a_{in}^{(2)}(t)}{a_{in}^{(2)}(t) + K_M^{(1)}}$$

The system of equations (2) is essentially (1) for two different cell types with densities $n^{(1)}(t)$ and $n^{(2)}(t)$, periplasmic antibiotic concentrations $a_{in}^{(1)}(t)$ and $a_{in}^{(2)}(t)$, densities of lysed cells $y^{(1)}(t)$ and

$y^{(2)}(t)$. These two cell types share external environment which can be seen in the system of equations in two ways: $a_{out}(t)$ is the same for both cell types and logistic growth part ensures that the carrying capacity of nutrients is shared by two types evenly ($\gamma_g n^{(1)}(t)\left(1-\frac{n^{(1)}(t)+n^{(2)}(t)}{n_{max}}\right)$ and $\gamma_g n^{(2)}(t)\left(1-\frac{n^{(1)}(t)+n^{(2)}(t)}{n_{max}}\right)$ terms).

1.2 Solutions in various limits

In order to get some intuition about model prediction for the inoculum effect curve of a single strain, we will consider the limits of small and large initial antibiotic concentration relative to the K_M of the enzyme. In section 1.2.1, we will derive the expression for the duration of the death phase of the bacterial growth for which $a_{out}(t=0) = MIC$. In sections 2.2.2 and 2.2.3, we will derive the expression for the inoculum effect curve in the limits of low and high initial antibiotic concentrations $a_{out}(t=0)$ respectively.

1.2.1 Death and growth time

In our model, the cells either grow exponentially or die exponentially. Assuming that initial cell density is n_0 and final cell density at $t_{20} = 20\ hours$ is n_f (which is fixed in the MIC experiment), we can write the following system of linear equations on the time intervals when the culture dies t_{death} and the time interval when the culture grows t_{growth}:

$$t_{death} + t_{growth} = t_{20}$$

$$\gamma t_{growth} - \gamma_d t_{death} = ln(n_f/n_0)\ .$$

with the solution for t_{death}

$$t_{death} = \frac{\gamma t_{20} - ln\left(\frac{n_f}{n_0}\right)}{\gamma_d + \gamma}.$$

1.2.2 $a_{out}(t = 0) \ll K_M$

Then $a_{out} \ll K_M$ and $a_{in} \ll K_M$ for all t, and

$$a_{out} = a_{in}(\frac{V_{max}}{CK_M} + 1)$$

Next, while $a_{out} > scMIC$ (the same as $a_{in} > scMIC_{Dh5\alpha}$),

$$n(t) = n_0 e^{-\gamma_d t},$$

$$y(t) = n_0(1 - e^{-\gamma_d t}).$$

Therefore,

$$\frac{da_{out}}{dt} = -n_0(1 - e^{-\gamma_d t})\frac{V_{max}}{K_M}a_{out} - n_0 e^{-\gamma_d t}(\frac{\frac{V_{max}}{K_M}}{1 + \frac{V_{max}}{CK_M}})a_{out}$$

with the solution

$$a_{out} = a_0 \exp(-\frac{n_0 V_{max}(CK_M t + \frac{e^{-\gamma_d t}V_{max}}{\gamma_d} + V_{max}t)}{K_M(CK_M + V_{max})}). \quad (3)$$

Plugging in $a_0 = MIC$, $a_{out}(t = t_{death}) = scMIC$,

$$ln(\frac{MIC}{scMIC})$$

$$= \frac{n_0 V_{max}((CK_M + V_{max})(\gamma t_{20} - ln(\frac{n_f}{n_0}))/(\gamma_d + \gamma) + \frac{\exp(-\gamma_d(\gamma t_{20} - ln(\frac{n_f}{n_0}))/(\gamma_d + \gamma))V_{max}}{\gamma_d})}{K_M(CK_M + V_{max})}.$$

For the parameter values that we have, we can ignore the exponent at the right-hand side and logarithmic dependence on n_0:

$$MIC \propto scMIC\exp(\frac{n_0 V_{max}}{K_M}\frac{\gamma t_{20}}{\gamma_d + \gamma}). \quad (4)$$

Thus, at low initial antibiotic ($MIC \ll K_M$), MIC increases exponentially with the increase of n_0.

1.2.3 $a_{out}(t = 0) \gg K_M$

Typically, $scMIC \leq K_M$, so the initial antibiotic concentration is much higher than scMIC and the cells initially die. In order for initial antibiotic concentration to be an MIC, the death phase should be significantly long (otherwise, the regrowth will happen faster than in 20 hours). This fact together with an observation that $a_{in} \leq a_{out}$ allows us to disregard the antibiotic hydrolysis inside the cell and only consider hydrolysis outside:

$$\frac{da_{out}}{dt} = -n_0(1 - \exp(-\gamma_d t))V_{max}.$$

Note that we assume $a_{out} \gg K_M$ for all t, which is not the case when antibiotic is almost completely hydrolyzed.

$$a_{out} = a_0 - n_0 V_{max}(t + \frac{\exp(-\gamma_d t)}{\gamma_d})$$

Whenever a_{out} becomes comparable to K_M, a_{out} starts to be broken exponentially in time. However, in the limit of high enough a_{out}, this time of exponential hydrolysis will be much smaller than the time of linear hydrolysis (3).

Plugging in (3) $a_0 = MIC$, $a_{out}(t = t_{death}) = scMIC$,

$$scMIC = MIC - n_0 V_{max}(\gamma t_{20} - ln(\frac{n_f}{n_0}))/(\gamma_d + \gamma).$$

Ignoring the logarithmic term,

$$MIC \propto scMIC + n_0 V_{max} \frac{\gamma t_{20}}{\gamma_d + \gamma}.$$

Thus, at high initial antibiotic concentrations ($a_{out} \gg K_M$), MIC increases linearly with the initial cell density n_0.

1.3 Generality of scMIC: growth rate as a function of internal antibiotic concentration

In the derivations above, we assume that the growth rate is a step function of antibiotic concentration: $\gamma(a_{out}) = \gamma$ for $a_{out} < MIC$ and $\gamma(a_{out}) = -\gamma_d$ for $a_{out} < MIC$. However, $\gamma(a_{out})$ can be any weakly decreasing function. The concept of scMIC is general and useful for various functions $\gamma(a_{out})$. The following statements hold as long as resistance mechanism is cooperative:

1. The general scaling of MIC* as a function of initial cell density are independent of the exact functional form of (a_{out}):

(a) MIC* scales exponentially with the initial cell density when smaller than K_M;

(b) MIC*scales linearly with the initial cell density when larger than K_M .

2. scMIC is well-defined because the inoculum effect curve asymptotically approaches a limit at small initial cell densities.

1.4 Small cell densities

The term "small (initial) cell densities" that we are using corresponds to the dilute conditions, when the cooperative part of the resistance is very weak. From equation (4), the dilution condition is as follows:

$$\frac{n_0 V_{max}}{K_M} \frac{\gamma t_{20}}{\gamma_d + \gamma} \ll 1,$$

which under conservative assumptions (see 1.5) of $K_M = 10\mu g/ml$, $V_{max} = 10^4 \mu g/ml$ per hour per OD results in the following condition:

$$n_0 \ll 2 \cdot \frac{10^4 cells}{ml}.$$

1.5 Parameter values

Parameter	Value	Justification
C	23.4 per hour per OD	Inoculum curve fit
γ	1.4 per hour	Experimentally measured
γ_d	2 per hour	Experimentally measured
MKC_{Dh5a}	0.03 μg/ml	Experimentally measured
$n_{\max}$	1 OD	Experimentally measured

Strain dependent:

Parameter	Value	Justification
TEM-20 Vmax	8400 μg/ml per hour per OD	Inoculum curve fit
TEM-52 Vmax	78000 μg/ml per hour per OD	Inoculum curve fit
TEM-20 Km	17.28 μg/ml	Inoculum curve fit
TEM-52 Km	16.56 μg/ml	Inoculum curve fit

While C may seem to be another parameter to the inoculum curves fit, it has a constraint that it should be the same for several inoculum effect curves. Thus, every inoculum effect curve except for one has two free parameters in their model fits.

2 The model with the enzyme degradation

While the simple model presented in section of this chapter explains qualitatively the behavior of the system at low antibiotic concentrations, it fails to explain some properties of the system at high antibiotic concentrations. There are two major discrepancies:

1. Inoculum effect curve, high cell densities and high MIC*. The data points are not only always lower than the model prediction, but also suggest different scaling of MIC* as a function of initial cell density than the model.

2. Competition data, high antibiotic concentrations. The data suggests that there is a second peak of selection for the more resistant strain at high antibiotic concentration, while the simple model suggests that above the scMIC of the more resistance strain, selection level relaxes to some level with no dips or peaks.

The discrepancies above happen in different experiments under similar conditions - at high initial antibiotic concentrations. This is why it might be the case that they happen for the same reason. We have considered several ways in which our model can be modified, out of which introducing beta-lactamase degradation turned out to be the most promising one.

The enzyme degradation may happen on its own and because of the reversible substrate-induced inactivation (Bonomo & Tolmasky, 2007). In the model below, we make two assumptions:

1. Different enzymes have different degradation rate in the absence of antibiotic.

2. The degradation rate of an enzyme is a linear function of antibiotic concentration - the higher antibiotic concentration, the higher the degradation rate.

Generally, as long as inhibition changes V_{max} as a function of antibiotic concentration, the scaling of the inoculum effect curve at high antibiotic concentrations should become sublinear. That means that if the inhibition is accounted for it takes longer to inactivate the antibiotic to the level of scMIC than without inhibition and the effect of inhibition is larger at high antibiotic concentrations, which makes the selection increase the second time at high antibiotic concentrations.

Given two observations above, we constructed a model, which incorporates the degradation rate of beta-lactamase, linearly proportional to the cefotaxime concentration.

$$\frac{\mathrm{d}a_{out}(t)}{\mathrm{d}t} = -Cn(t)(a_{out}(t) - a_{in}(t)) - y(t)\frac{V_{max}a_{out}(t)}{a_{out}(t) + K_M}$$

$$\frac{\mathrm{d}n(t)}{\mathrm{d}t} = \begin{cases} \gamma n(t)\left(1 - \frac{n(t)}{n_{max}}\right), & a_{in} < scMIC_{Dh5\alpha} \\ -\gamma_d n(t), & a_{in} \geq scMIC_{Dh5\alpha} \end{cases}$$

$$\frac{\mathrm{d}y(t)}{\mathrm{d}t} = \begin{cases} -\alpha y(t)a_{out}(t), & a_{in} < scMIC_{Dh5\alpha} \\ -\frac{dn(t)}{dt} - \alpha y(t)a_{out}(t), & a_{in} \geq scMIC_{Dh5\alpha} \end{cases}$$

$$C(a_{out}(t) - a_{in}(t)) = \frac{V_{max}a_{in}(t)}{a_{in}(t) + K_M}$$

where α - the enzyme degradation rate per unit of antibiotic concentration. Figure 8 shows the fits of the inoculum effect curves and the model prediction for competition experiments for $\alpha_{TEM-20} = 0.003(hour\frac{\mu g}{mL})^{-1}$ and $\alpha_{TEM-52} = 0.001(hour\frac{\mu g}{mL})^{-1}$. The other parameters stay the same as in the main text fits.

3 Summary of all strains used in the study

All the strains used in the study are identical except for the beta-lactamase gene and abscent/present flourescent protein producing plasmids. These plasmids may or may not be present in the strains depeding

on whether the experiment requires flourescent labeling. The table below summarizes various strain types based on their beta-lactamase gene and relate the version of the gene to TEM-1.

Name(s) used in text	Mutations from TEM-1	scMIC in cefotaxime
reference strain, TEM-20	M182T,G238S	0.65
mutant strain, TEM-52	E104K,M182T,G238S	8
A42G mutant of TEM-20	A42G,M182T,G238S	1.78
TEM-15	E104K,G238S	1.59
TEM-19	G238S	0.22
A42G mutant of TEM-17	A42G,E104K	0.11

4 Sequencing summary

Below is the summary of the mutations observed in the end of the evolution experiment (Fig 1c and S4).

Starting strain	Evolving antibiotic concentration, $\mu g/mL$	Final scMIC, $\mu g/mL$	Mutation observed	Comments
TEM-19	0.06	0.25	Promoter AACCCTGAT->AAACCTGAT, L12F	Could not find any information
TEM-19	0.25	0.5	observed	

			synonymous mutation at position 20 GCC->GCT	
TEM-19	0.5	1	A184V	A known mutation which is present in TEM-116, TEM-157, TEM-162, TEM-181, TEM-187 and TEM-119 (Jacoby, 2006).
TEM-20	0.7	0.7	Promoter AACCCTGAT->AAACCTGAT	
TEM-20	0.17	0.7	AACCCTGAT->AAACCTGAT 50-50	
A42G mutant of TEM-17	0.25	5.7	G238A; L12F	G238A has been constructed before, demonstrated increase in k_{cat} and decrease in K_M [cantu1998role]. Some mutations at

				12th position have been observed, but not to F (Demanèche *et al*, 2008).
A42G mutant of TEM-17	0.25	0.5	G238S	This is a well-established mutation known to increase resistance to cefotaxime. (Weinreich *et al*, 2006)
A42G mutant of TEM-17	0.45	4	G238S	This is a well-established mutation known to increase resistance to cefotaxime. (Weinreich *et al*, 2006)

5 Figures for chapter 3

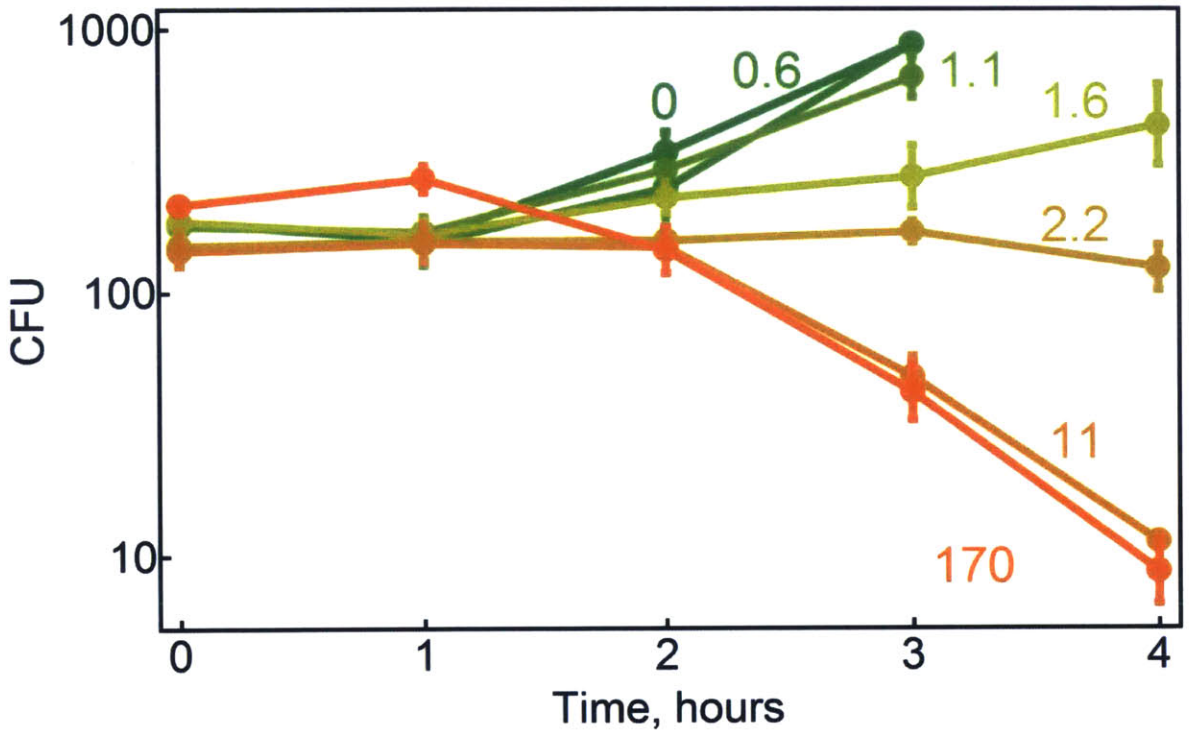

Figure S1. Growth rate can be modeled as a step function of external antibiotic concentration. The transition between exponential growth with the highest growth rate and exponential death with the highest death rate is relatively sharp. Different colors correspond to different antibiotic concentration. A42G mutant of TEM-20 is used, the measured scMIC of this strain is 1.6 $\mu g/mL$, the measured MIC is 64 $\mu g/mL$. For this figure, the bacterial were cultured in 50 mL flasks and at the measurement time point some dilution of bacteria were plated. The error bars correspond to the square root of the CFU.

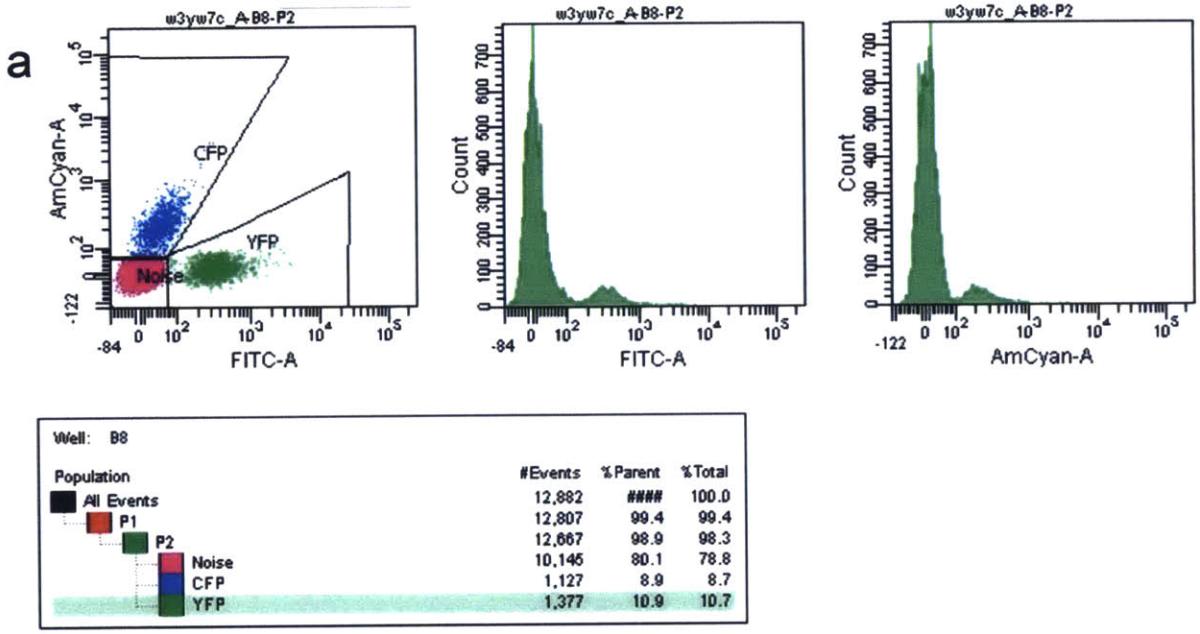

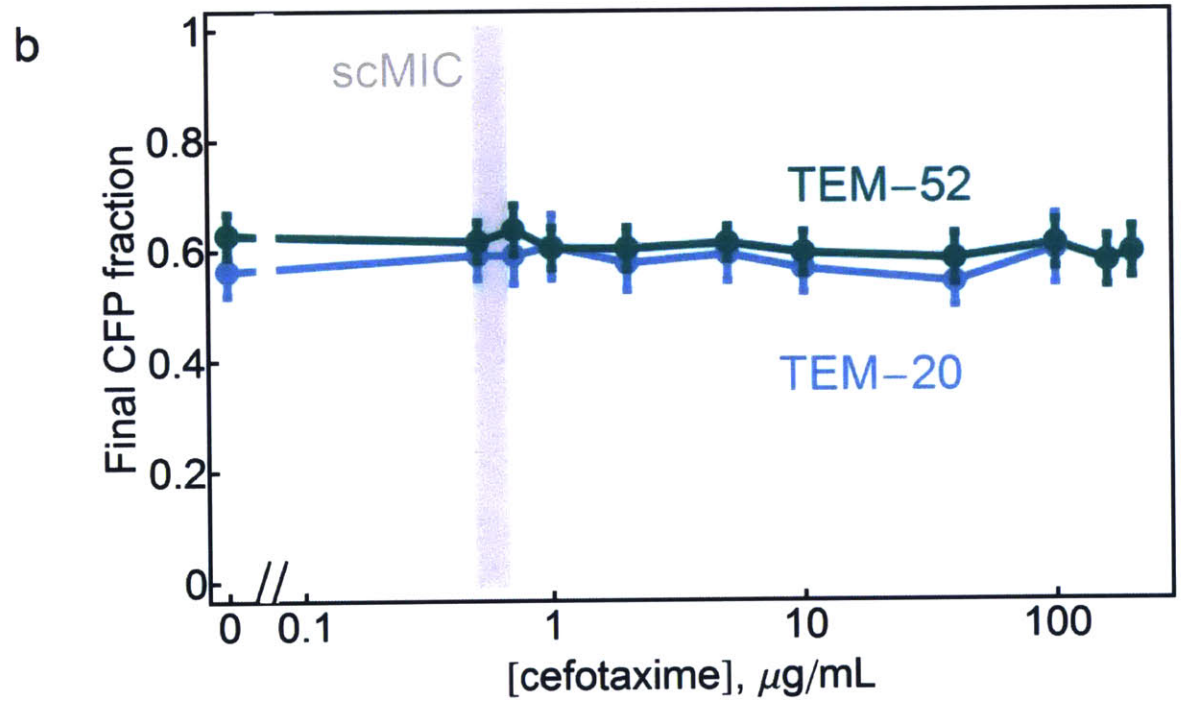

Figure S2. Flow cytometry fraction measurements (a) YFP (x-axis) and CFP (y-axis) signals on one plot

and histograms of the YFP and CFP counts. (b) TEM-20 and TEM-52 strains of different colors competing. The fraction of CFP variant of the strain stays flat as a function of antibiotic concentration. This figure proves that selection patterns observed in the main text are not due to the influences of cefotaxime presence on kanamycin plasmids.

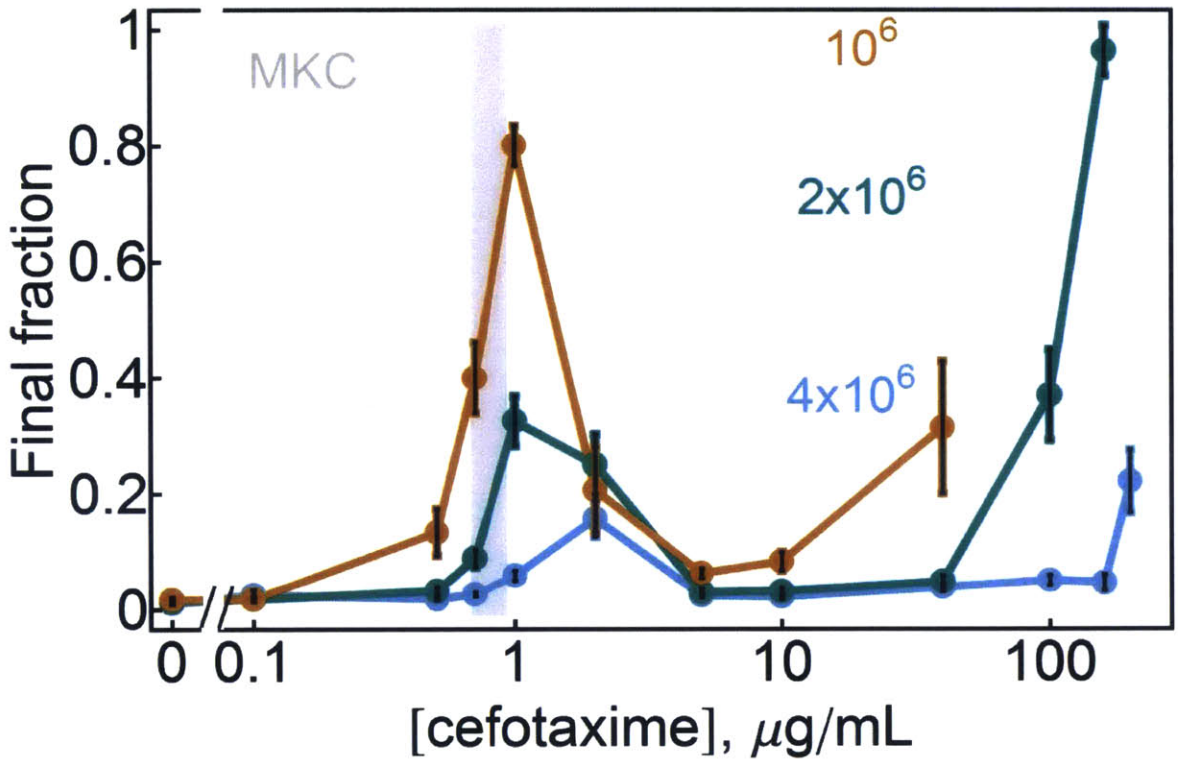

Figure S3. In competition of TEM-20 and A42G mutant of TEM-20, selection for the mutant begins at the scMIC, not MIC*, of TEM-20. For most of the data points, the mean values for 8 different cultures with different coloring of the strains are presented. The error bars are the standard error of the mean. The gray bars correspond to the scMIC value of TEM-20. The scMIC and MIC* of TEM-20 are 0.8 $\mu g/mL$ and 14.3 $\mu g/mL$ correspondingly, the MKC and MIC* of A42G mutant of TEM-20 are 1.59 $\mu g/mL$ and 64 $\mu g/mL$ correspondingly.

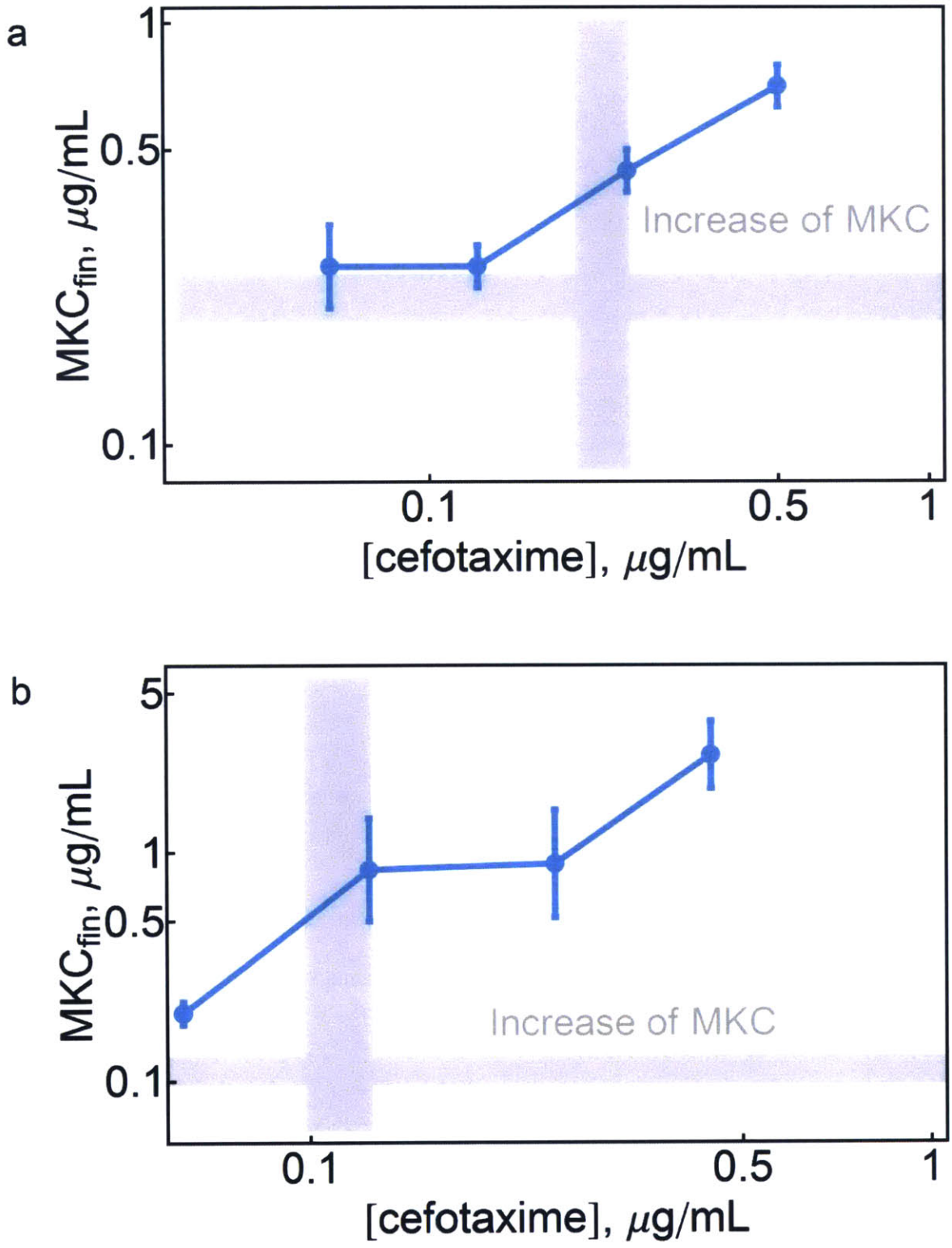

Figure S4. Laboratory evolution experiments of (a) TEM-19 and (b) A42G mutant of TEM-17 confirm

that increase of resistance evolves in antibiotic concentrations equal to and larger than the scMIC. Plotted is the scMIC measured after 13 days (~100 generations) versus the concentration of cefotaxime the strains were evolved at. The error bars are the standard errors of the mean of six independent evolved populations. The gray bars correspond to the initial scMIC values.

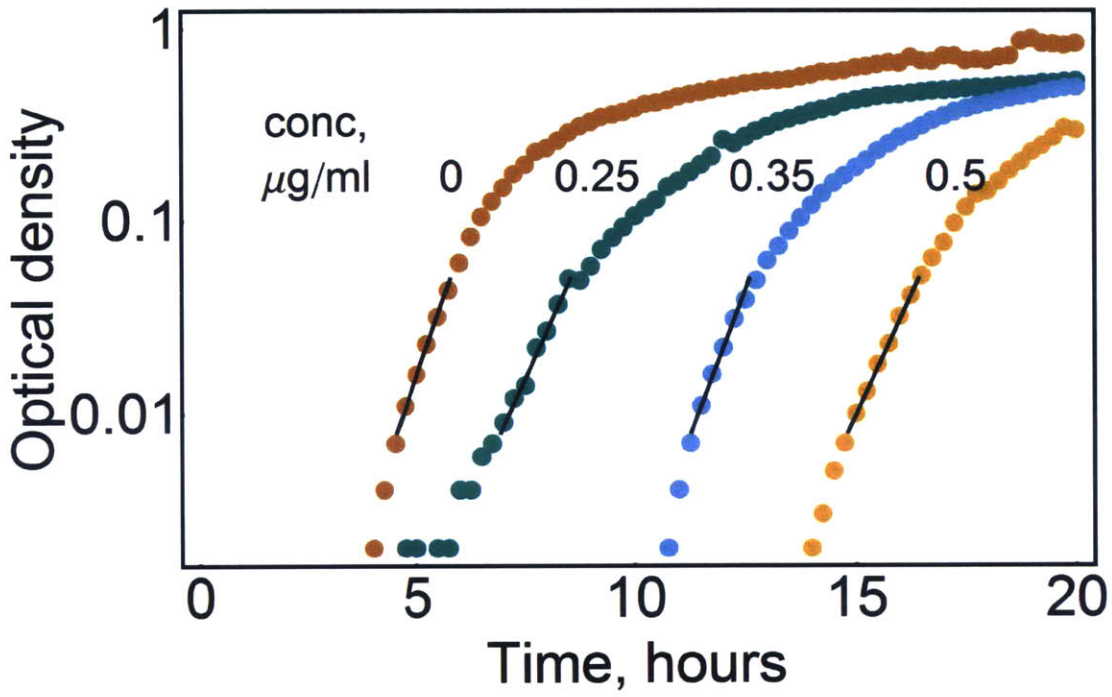

Figure S5. Growth curves of TEM-20 in different antibiotic concentrations. With the increase of antibiotic concentration, the slope of the growth curves does not change, while the time to reach some optical density increases. This is a result of the cooperative growth: the cells first cooperatively hydrolyze cefotaxime and then grow with maximal division rate.

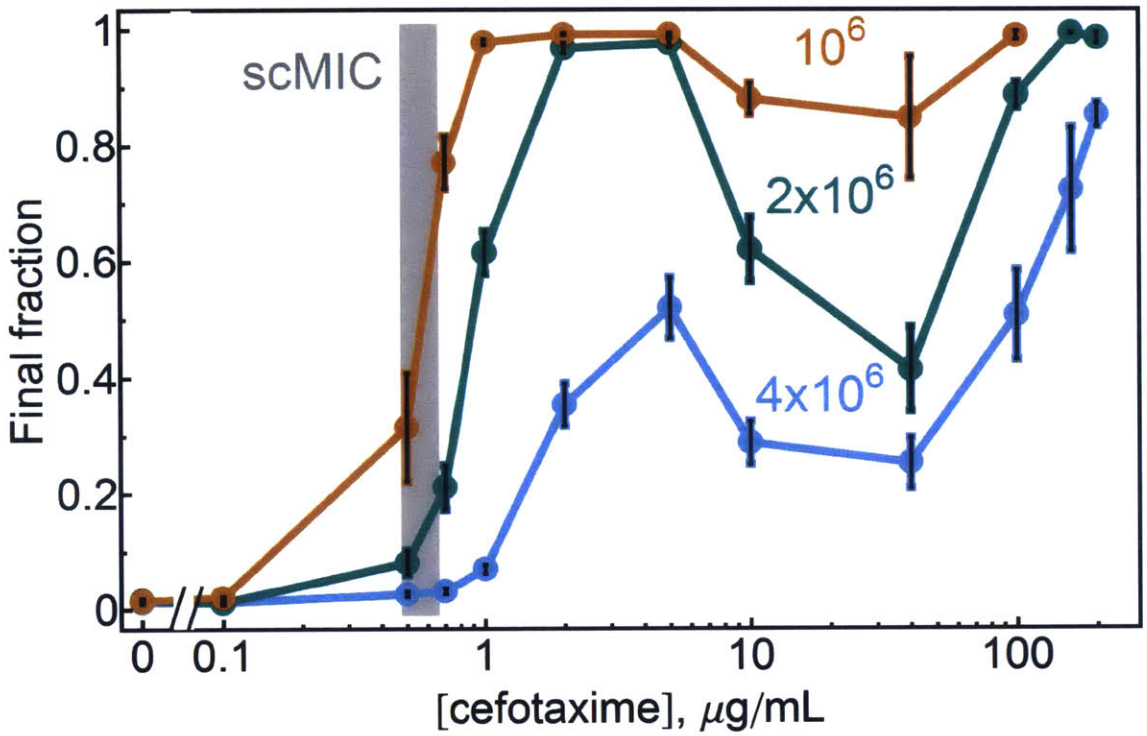

Figure S6. The experimental data for competition experiments, with a 1% initial fraction of the mutant strain. At the scMIC of the reference strain, the final fraction of the mutant starts to increase, indicating that selection for the more resistant mutant starts near the scMIC. Different colors correspond to different initial cell densities (labeled in CFU/ml). The error bars are the standard error of the mean (n = 9 – 10 for most data points). The gray bar corresponds to the scMIC of the reference strain. For the model, parameter values are provided in section 1.5 of this chapter.

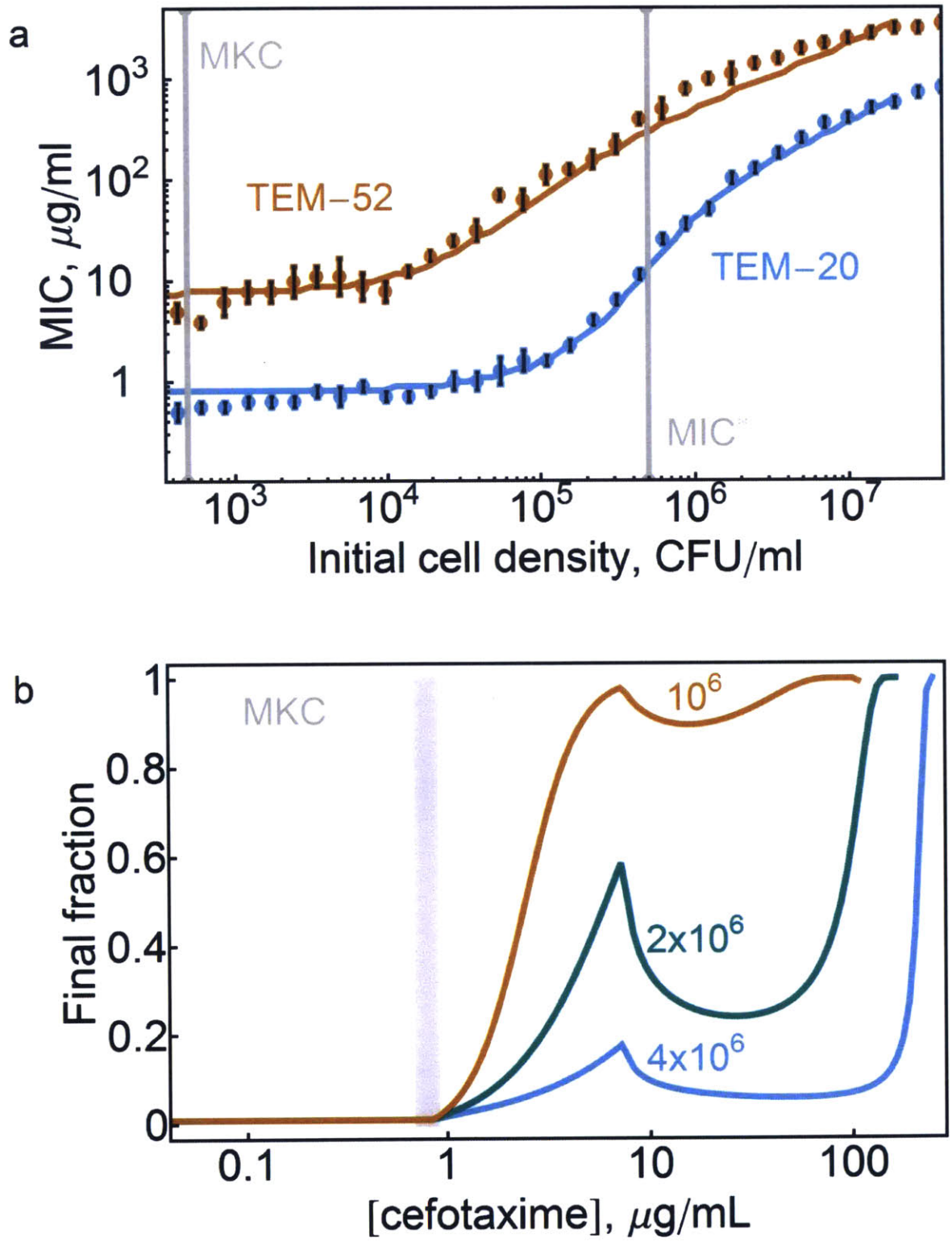

Figure S7. The model with the enzyme-cefotaxime irreversible binding explains the inoculum effect and

also the selection patterns at high antibiotic concentrations. (a) The fits of the inoculum effect curves of TEM-20 and TEM-52. The error bars are the maximum of a discretization error and the standard error of the mean of three measurements. (b) The model prediction for competition experiments, with a 1% initial fraction of TEM-52. At high antibiotic concentrations, the second selection peak appears. The parameter values used can be found in sections 1.5 and 2. Different colors correspond to different initial cell densities (labeled in CFU/ml). The gray bar corresponds to the scMIC of TEM-20.

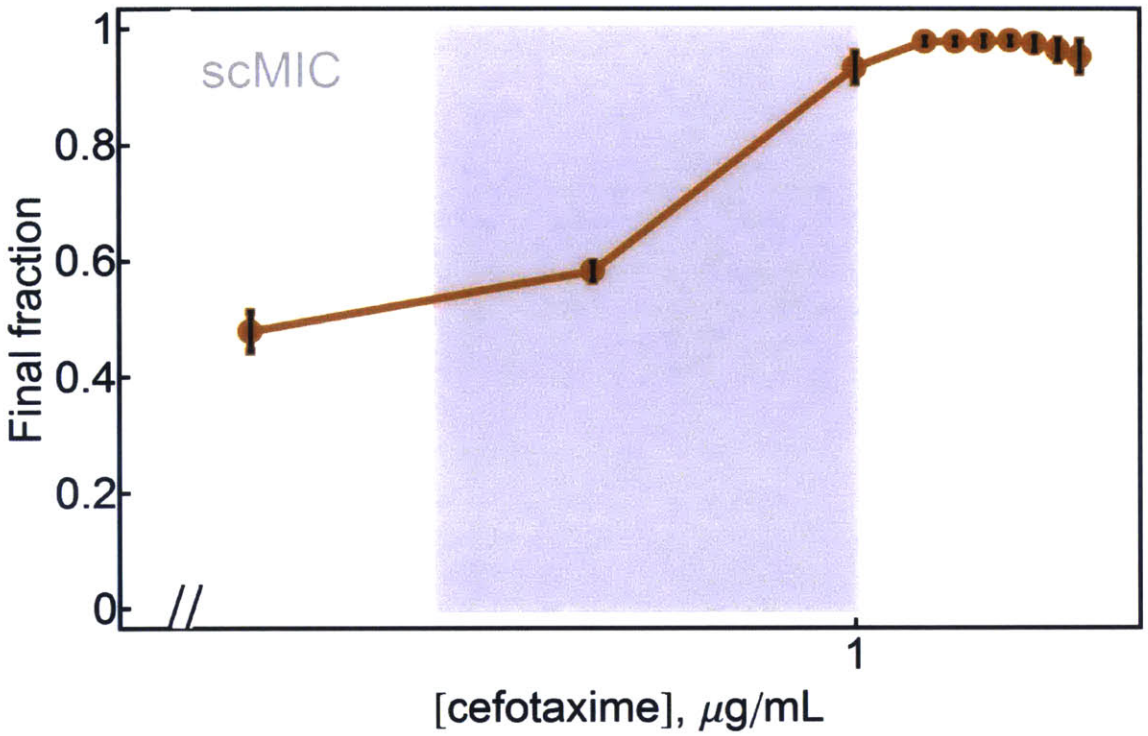

Figure S8. Selection favors an increase of scMIC not MIC*. The competition experiment of TEM-15 and the A42G mutant of TEM-19 (initial fraction plotted as horizontal line, initial cell density 5x10^5 cells/ml). TEM-15 has a higher scMIC (1.78 $\mu g/mL$ vs 1.26 $\mu g/mL$), while both strains have similar MIC* values (18 $\mu g/mL$ vs 20 $\mu g/mL$, which are statistically indistinguishable, because the antibiotic dilution factor is $\sqrt{2}$). For cefotaxime concentrations above the scMIC of the A42G mutant of TEM-19, the TEM-15 strain is selected for, indicating that selection maximizes the scMIC rather than the MIC*. Error bars are the standard errors of the mean of 4 independent populations.

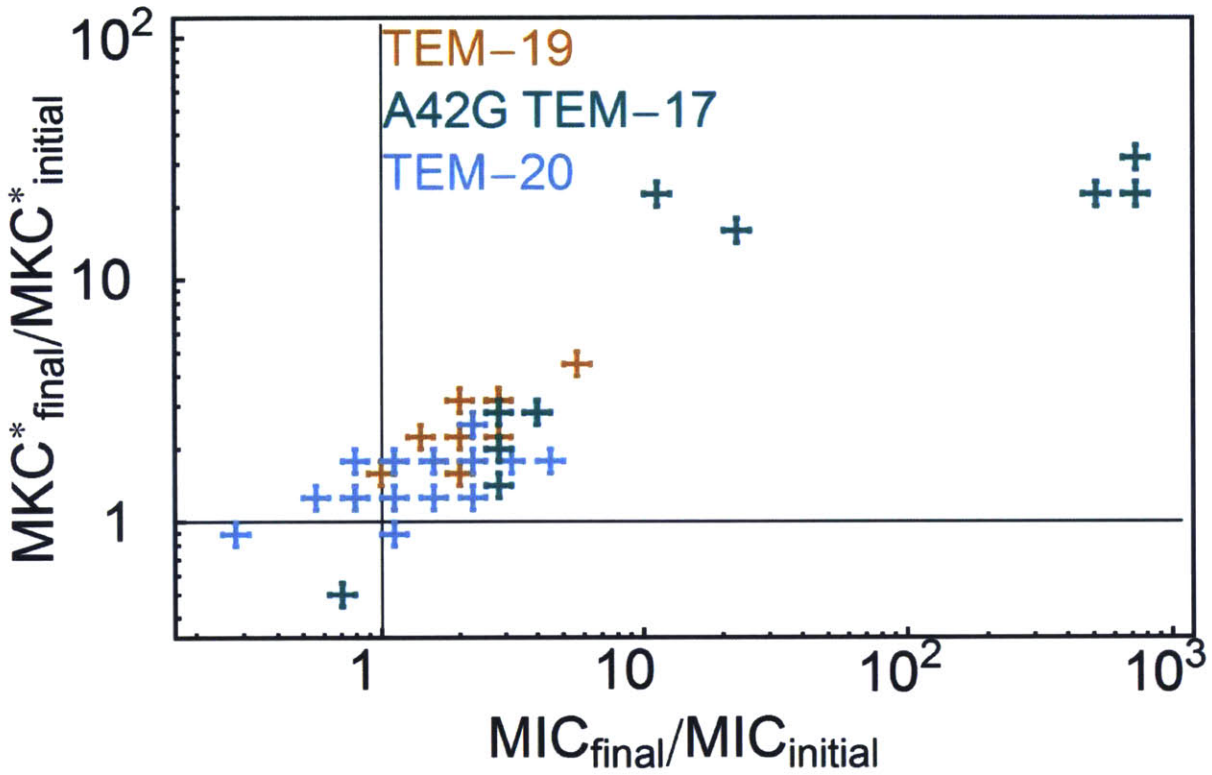

Figure S9. Sometimes an increase in scMIC is accompanied by the decrease in MIC*. The scMIC vs MIC* values of the evolved cultures as a fraction of the initial scMIC or MIC* values are presented. Only data for the cultures evolved at concentrations equal to or greater than the scMIC of the initial strain is shown. Different colors correspond to different strains evolved. The data presented is the same as in Fig. 1c and S4.

Chapter 4. Selection in expanding populations follows universal behavior.

Natural populations acquire new territories through a process of expansion. One prominent example of this process is the migration of humans out of Africa(Templeton, 2002). Another well-known example is the colonization of Australia by cane-toads(Phillips *et al*, 2006). When studied in the lab, invasion is usually modeled by bacterial colony expansion on the surface of agar in a petri dish. During this invasion of new territory there will also typically be many opportunities for evolutionary change as the population expands. For the case of the human expansion, one of the contemporary observable outcomes of the expansion is a gradient of skin and hair color from Africa to Northern Europe. It is believed that the change was occurring as a response to the amount of the ultra-violet radiation making certain amount of pigments most advantageous for certain areas. In other words, the gradient in the trait corresponds to the gradient in the environment. For the case of cane toads, there has been observed a gradient in the length of the legs the further they are from the coast. While certainly there is a gradient in the environment from the coast to the interior of the continent, there is also evidence that the length of the legs is correlated with the invasion speed. Therefore, the gradient is likely the result of the selective pressure to increase speed during the expansion.

Understanding the evolutionary dynamics of expanding population is a fundamental problem because it is one of the major forces that shape contemporary diversity of natural populations. While there are many different models that describe expanding populations, one of the simplest and most widely used is Fisher-Kolmogorov equation (Fisher, 1937)(Kolmogorov *et al*, 1937)(Fig. 1a). In this model, it is assumed that local population density grows logistically and that over sufficiently long length and time scales the motility of individuals can be described by diffusion. This reaction-diffusion model then connects the parameters characterizing the behavior of individuals such as growth rate and migration rate with the population-scale parameters such as the velocity of expansion and the shape of the expansion front. In

particular, the growth rate and diffusion coefficient at small population densities completely determine the expansion.

The Fisher equation is easily generalized to the case of competing genotypes by assuming that both subpopulations share resources and collectively can only grow to a certain density (Fig. 1d). In this situation the more fit genotype will spread locally but will also spread through the population spatially. Interestingly, this local spread occurs even if the more fit population has a lower growth rate; this perhaps counter-intuitive prediction is because fitness in an expanding population corresponds to the velocity of the population wave (when the genotype is alone), which in the Fisher model is proportional to the product of the genotype's division rate and diffusion coefficient at low density. Selection in spatially expanding populations therefore has a richness that is not present in well-mixed populations.

To develop a theoretical expectation of how the selective process should behave in a population expanding as a Fisher wave, we started by performing simulations and analytic calculations of how the ratio of two genotypes behaves during a range expansion. We found that this ratio depends exponentially on the spatial coordinate along which the expansion is happening. The characteristic length of this exponent depends on the division and motility rates of the two genotypes – the more advantage one has over the other, the faster their ratio changes. While the details are introduced in the chapter 5, the intuition behind this observation is as follows. The interaction of the two waves is realized through the carrying capacity (the sum of the two densities at any point cannot be greater than the carrying capacity). Therefore, at the tip of the expanding wave where the densities are very small, the interaction does not matter. Then, in the frame of reference moving with the velocity of the expansion (either of the two expansions, as the two expansion velocities are assumed to be nearly equal because delta g is small), the faster growing wave can be interpreted as another Fisher wave with the same diffusion constant and deltag growth rate. It has been shown previously that the expansion of the Fisher wave is determined by the behavior of the front and does not matter on the details in the bulk of the wave(Hadeler & Rothe, 1975). Therefore, the exponent of the tip of the fraction Fisher wave will result in the exponential

dependence on the coordinate in the reference, non-comoving, frame. This exponential dependence of genotype fractions on position is predicted to be independent of whether the selective sweep occurred as the result of an increase in growth rate, increase in motility, or both. The Fisher model therefore predicts a remarkably simple pattern of genotype abundance both during and after the population expansion. Just as a more fit genotype spreads exponentially with time in a well-mixed population, a more fit genotype is expected to spread exponentially with space in a spatially expanding population (Fig 1 b,c).

The Fisher model, however, is only a special case of a wide class of models that describe expanding populations. The growth rate and diffusion coefficient can be any function of the cell density, potentially corresponding to a cooperatively growing population and/or density dependent diffusion. We find that under quite general assumptions, the exponential dependence of the ratio on spatial coordinate holds true. While the details can be found in Chapter 5, the general conclusion is that the quantity of the exponential length scale can depend on the model while qualitatively all models predict the fraction to be an exponential function of coordinate. Thus, the theoretical prediction is that under a wide range of assumptions, independent of the specific diffusion and growth processes shaping the expansion profile, selection in expanding populations is expected to display universal properties: the ratio of genotype frequencies is predicted to have an exponential dependence on position.

Experimentally, to the best of our knowledge, the existent studies either analyzed the existing natural population data (Phillips *et al*, 2006) or studied the microbes spreading on the surface of the agar(Hallatschek & Nelson, 2010). The first type of study is an important attempt to understand the genotypic and phenotypic diversity that we observe in natural populations. However, often not only the process of expansion influences this diversity but also the adaptation of the populations to new environmental conditions after they have expanded, which makes the analysis complicated. On the other hand, microbes spreading on the surface of agar generate reproducible results and can be controlled in many ways but have very small effective population sizes at the front, precluding study of the selective process occurring during the population expansion.

To explore our theoretical predictions of universal behavior during selection in expanding populations, we use populations of the motile bacterium *E.coli* expanding in soft agar. *E. coli* moves through a process of semi-straight runs interspersed by occasional tumbles that randomize the direction that the cell is swimming. In the absence of attractants and repellants this motility results in behavior that is usually modeled as a random walk, and in the limit of many runs and tumbles, diffusion. When attractants or repellants are present, the runs in unfavorable directions become shorter, resulting in a biased random walk (or diffusion with drift).

We find that our E. coli populations indeed expand though the soft agar as a population wave that depends upon both motility and cell division. We used bacteria with a single plasmid conferring resistance to an antibiotic and producing a fluorescent protein. We used two types of plasmid: kanamycin resistant plasmid that also produces red fluorescent protein and ampicillin resistant plasmid that produces yellow fluorescent protein. We find that bacterial populations carrying these two plasmids expand with different velocities (Fig. 2b). Importantly, after an initial transient each population has a constant velocity, suggesting that the two strains have a well-defined fitness in the context of an expanding population. The shape of the population front was not consistent with the Fisher prediction (Fig. 2a), but as discussed previously we expect that the universal signatures of selection in expanding populations may nonetheless be observable.

To study the spatial behavior of selection in expanding populations we inoculated soft agar with a mixture of our two E. coli strains. After the population has expanded the 8cm of the lane and saturated the environment we sample from the agar every 0.5 cm using a multichannel pipette and analyze the population composition using flow cytometry. As predicted by our theoretical calculations, we found that the fraction of the mutant is indeed an exponential function of the spatial coordinate (Fig. 3d).

Next, we decided to characterize the fitness function of the expanding population. Fitness is the quantity that is maximized during evolution: if a mutant with higher fitness arises in the population, its fraction

increases over time until it either takes over the entire population or an even more fit mutant arises and starts to take over. We decided to use the analogy between liquid and soft agar environments again. In a well-mixed liquid environment, when two strains have equal fitness (i. e. growth rate), the fraction of either of them in the mixture stays constant over time. Therefore, by analogy, when the fraction of both strains in a mixture stays constant as a function of spatial coordinate in expanding populations in soft agar environment, the fitness of the two strains must be equal. Changing the kanamycin concentration when one of the two competing strains is kanamycin resistant and the other is not, will change the relative fitness of the two strains and therefore we can find the concentration when the two strains have equal fitness.

As discussed in the introduction, we expect that velocity should be the appropriate fitness metric in a spatially expanding population. The theoretical reason for this hypothesis is that the amount of individuals in a population under expansion scenario grows with the rate, proportional to the velocity of expansion. This is again analogous to the liquid culture exponential growth, when the rate of division of every individual cell is proportional to the growth rate, which is the fitness metric in liquid environment. To test this hypothesis, we measure velocities of the expansion of the two strains when exposed to kanamycin concentrations identical to those used in the competition experiment described above. Indeed, our preliminary results show that the kanamycin concentration at which velocities are equal falls in the range where competition does not necessarily favor one of the strains (Fig. 4). Velocity usually depends on both growth and motility, which makes it possible that the allele that has a slower growth rate nevertheless wins in the competition with the faster grower during the process of invasion of new territories.

During a real expansion, different alleles can confer different likelihood of starting to explore new territories, which is ignored by the discussion above. For example, it might be the case that the allele with the greater velocity requires more time before starting to expand. In bacterial population, it would correspond to a longer lag time. In the animal world, it may correspond to some physical barrier that

carriers of certain alleles overcome faster than other population representatives. In general, it is not uncommon to have tradeoffs such as growth rate and yield tradeoff in bacterial populations.

Experimentally we can manipulate the lag phase of an allele by delaying its introduction on the plate. We can also, as we described above, control the fitness difference between two strains by adjusting the kanamycin concentration. An interesting question can then be asked – is there any time delay that will prevent an otherwise more fit strain from spreading in the population? In the liquid well-mixed environment, the answer is no since during the lag time only the initial fraction of the strains will change. Under the scenario of a range expansion, however, it is hypothetically possible that a slower strain with a shorter lag time may be able to block the fitter allele from the new territory. Indeed, we find that the more fit strain can only take over if it is introduced into the environment within a critical "window" of time (Fig. 5). Therefore, lag time plays drastically different roles in spatially expanding populations and in well-mixed liquid environments. In expanding populations, it becomes vital for an allele to minimize its lag time.

It is not always possible to study natural populations while they expand. After the invasion of new territories, however, it may be possible to analyze spatial distribution of alleles to illuminate the selective process that took place during the range expansion. For instance, very often along the trajectories of expansion there are gradients of traits. Although it is usually thought to be the result of the gradients in the environmental conditions that facilitate gradients in adaptation, another origin of this pattern is selection during the process of expansion. In these cases, if available data is processed correctly, information about the expansion can be extracted. Here, we concentrate on the question of what kind of signals should one look for while working with the data available after populations have invaded new territories.

We argue that the emergence and spread of a new advantageous allele leaves a distinct pattern in the population long after it has invaded the new territory. This pattern is an exponential dependence of the

ratio of the two alleles on the spatial coordinate. We also show that qualitatively this pattern is universal across a wide range of assumptions about the mechanics of the population expansion. Quantitatively, it provides information about the expansion and theoretically can distinguish between different types of migration.

Figures

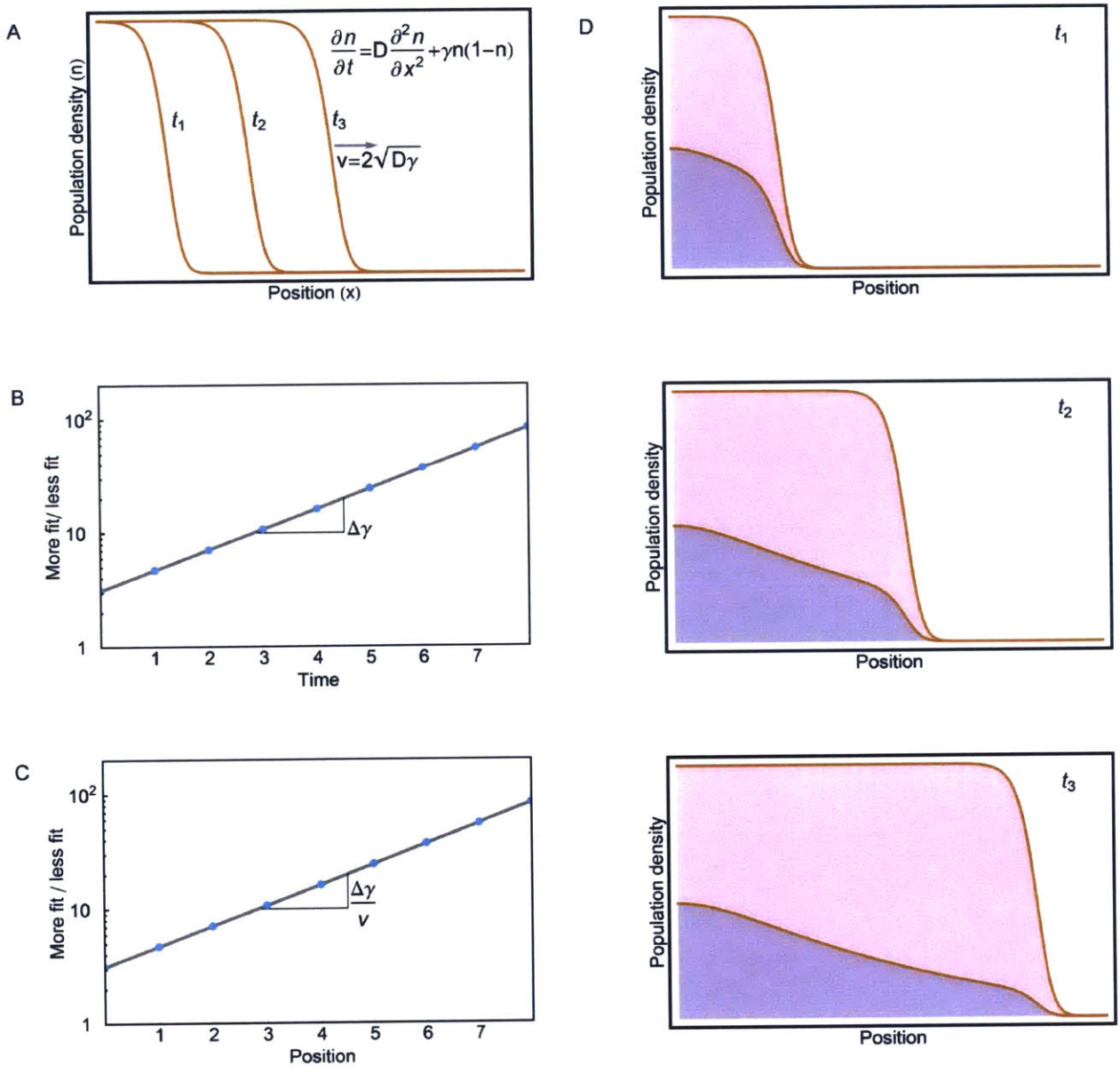

Figure 1. Fisher equation predicts that the ratio of two types is an exponential function of spatial coordinate (position). (a) The Fisher model predicts a population density profile of shown shape that expands with a constant velocity v. The profile is shown for three time points t1<t2<t3. (b) If two types compete in well-mixed environment, the fitter one takes over exponentially in time, and (c) if compete while expanding, exponentially in space. (d) At three time points, we show population composition. The

upper line correspond to total density of the two competitors, the lower line corresponds to the less fit phenotype population density.

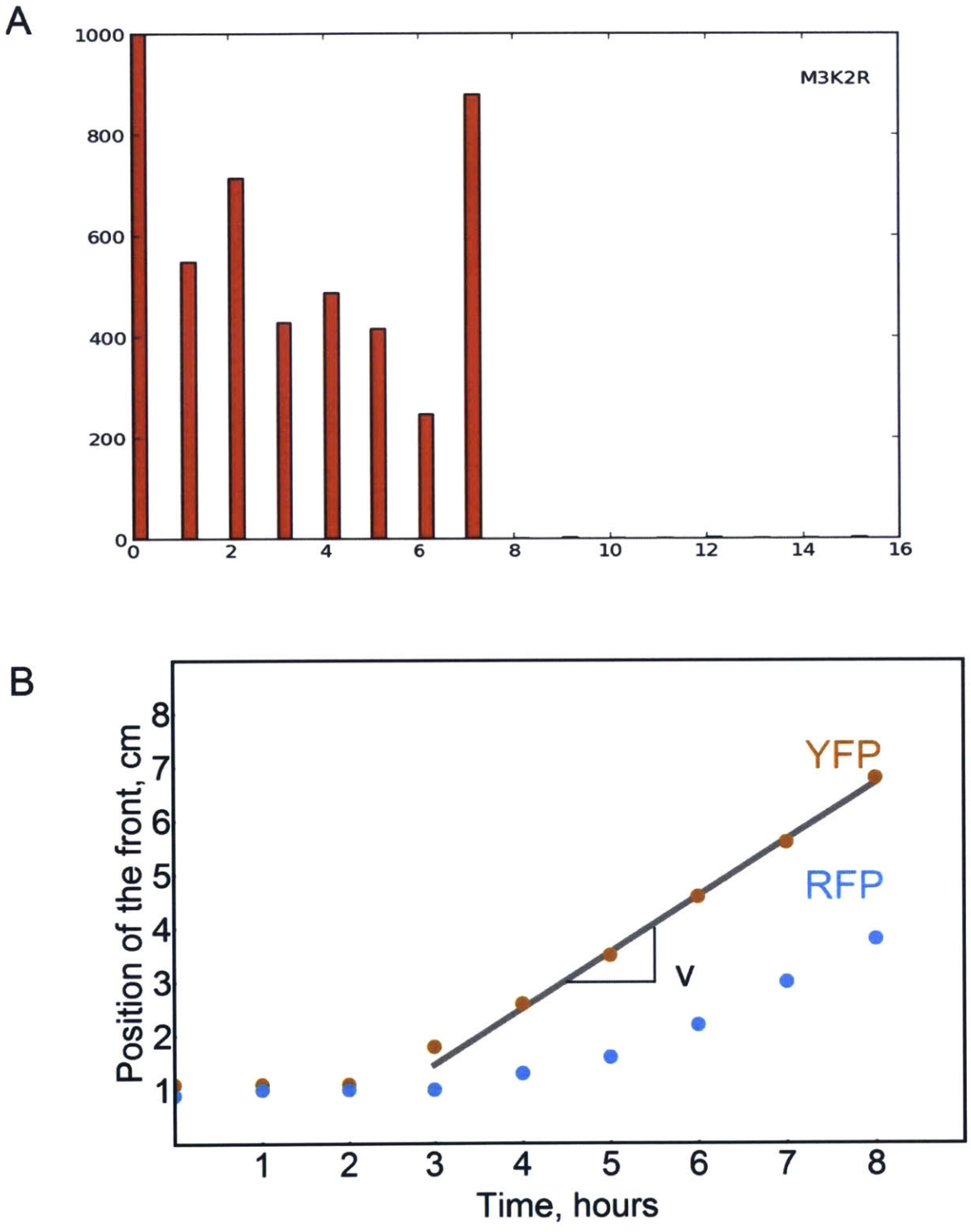

Figure 2. Expansion profile and velocity of bacteria in soft agar do not agree with Fisher model. (a) The

profile of expanding population wave as a function of sampling position. The distance between sampling positions is 0.5cm. The profile is non-monotonic and sharp for a given velocity. (b) The location of the front is a linear function of time after some initial lag phase, which means that the populations expand with a constant velocity. The velocity is the slope of the line.

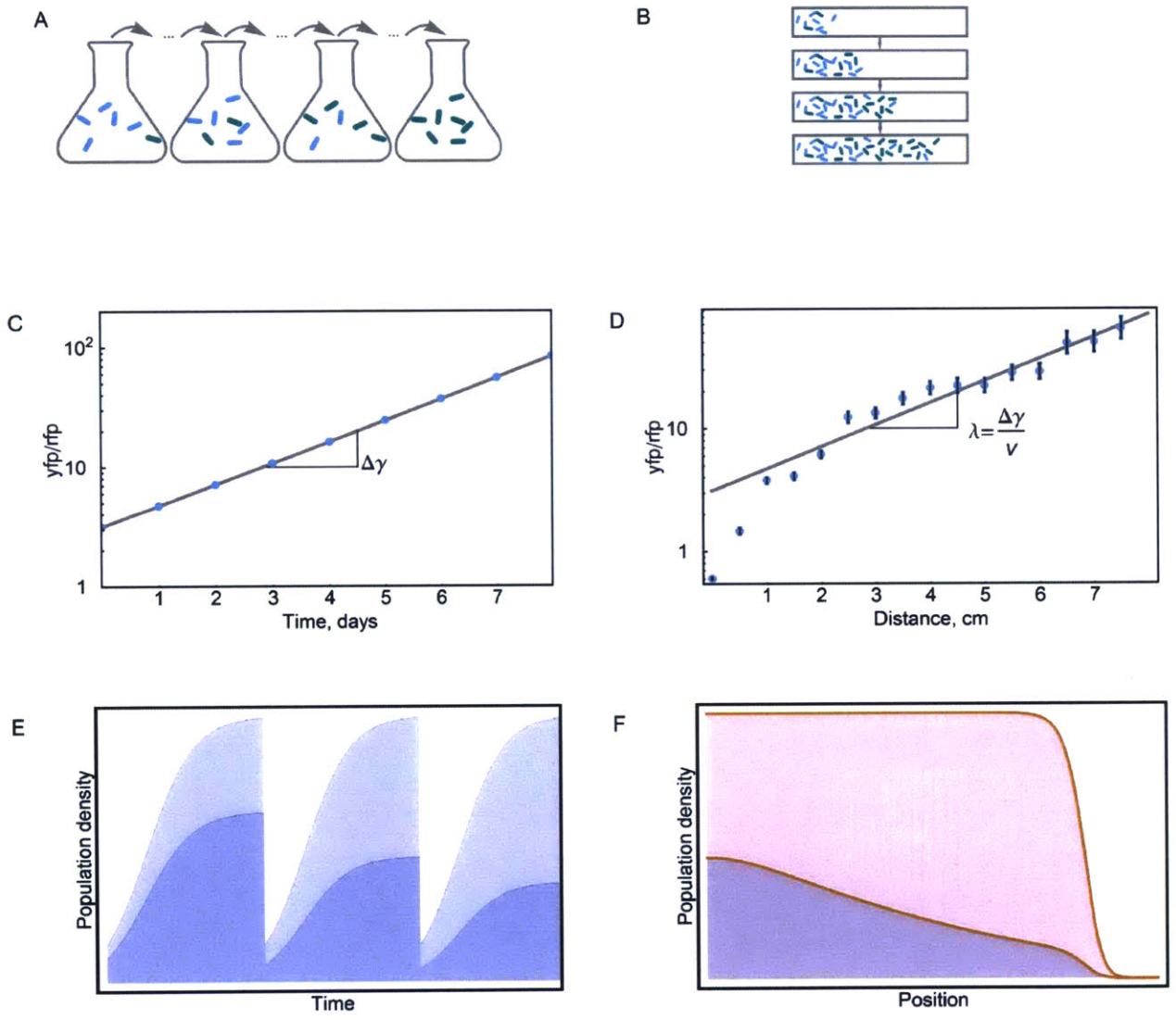

Figure 3. Similar to liquid culture, we observe a spatial exponent in real bacterial populations in soft agar. (a) schematic representation of liquid culture dilution experiment. Initially two strains are present – green and blue, bit with each dilution the more fit strain (green) becomes more abundant (b) schematic representation of spatial expansion experiment. Note that while in (a) arrows correspond to dilution steps, in (b) arrows correspond to a time difference. (c) A cartoon of competition experiment fake "data" in liquid. We expect the ratio of more fit strain to grow exponentially in time. (d) Data for spatial expansion

of bacteria in soft agar. After some transient period, the fraction of more fit strain depends on the coordinate exponentially. (e) and (f) correspond to the population composition as a function of time (e) and position (f) as predicted by simple models – logistic growth (e) and Fisher model (f). The lower curve corresponds to less fit strain.

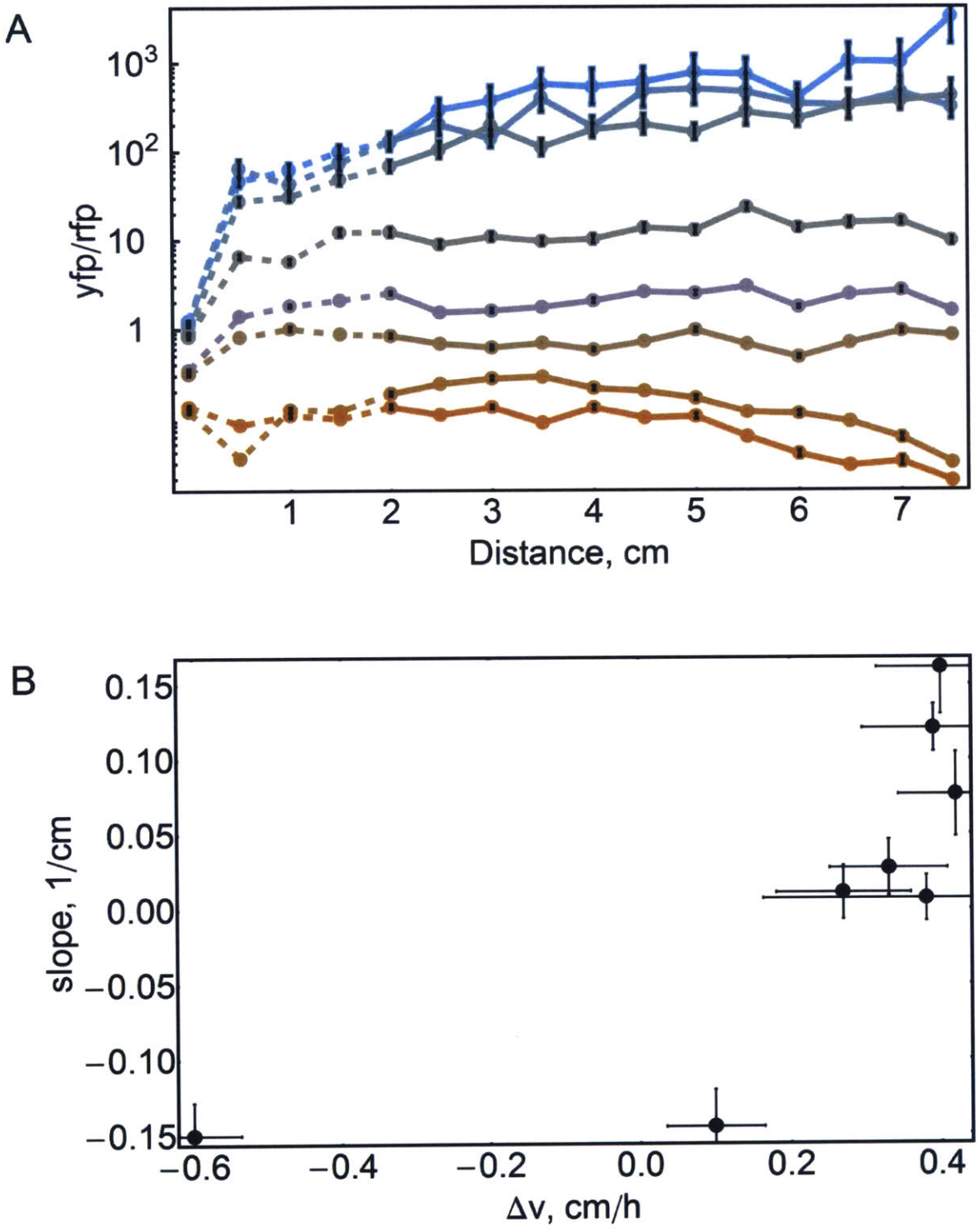

Figure 4. Kanamycin concentration controls the fitness difference of the two strains. (a) ratio of

kanamycin resistant to kanamycin sensitive strain had different spatial exponents for different kanamycin concentrations: 0,0.1,0.2,0.3 .. 0.7 following color gradient. Dashed parts of lines correspond to transient region, where the fraction equilibrates after inoculation to the plate in new environment. (b) Preliminary data do not contradict to the statement that velocity is a fitness of expanding population.

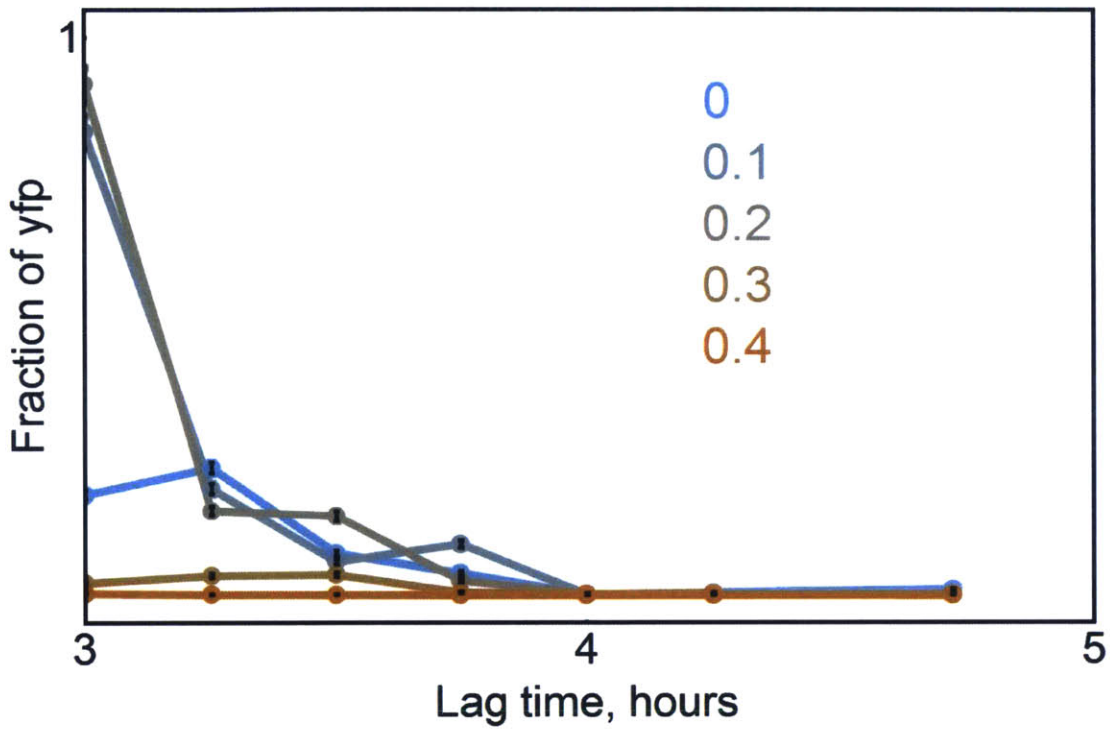

Figure 5: In spatially expanding population minimizing lag time is vitally important. The fraction of the more fit (YFP) strain is shown as a function of lag time – the time for which RFP cells were inoculated on the agar plate before YFP was added. With the increase if kanamycin concentration (legend), i.e the decrease of fitness difference, the critical lag time, after which YFP never catches up RFP, decreases.

Chapter 5 Supplemental to chapter 4

Competition of two strains in a well-mixed environment with daily dilution.

To model two growing in the well mixed environment during one day, we used the following system of equations:

$$\frac{dc_1}{dt} = \gamma_1 c_1(1 - c_1 - c_2)$$

$$\frac{dc_2}{dt} = \gamma_2 c_2(1 - c_1 - c_2)$$

Where c_1 and c_2 correspond to the densities of the two phenotypes. Each of them grows logistically with its own growth rate at small cell densities. The length of the day is T and is much larger than the division time.

We will make a substitution $c = c_1 + c_2$, $f = \frac{c_1}{c_1+c_2}$. Assuming $f \ll 1$, and keeping leading terms in f:

$$\frac{dc}{dt} = \gamma_2 c(1 - c)$$

$$\frac{df}{dt} = f(\gamma_1 - \gamma_2)(1 - c)$$

Solution to the first equation is $c(t) = \frac{1}{1+e^{\gamma_2 t}}$, therefore the equation for frequency the following:

$$\frac{df}{dt} = f(\gamma_1 - \gamma_2)\frac{e^{\gamma_2 t}}{1 + e^{\gamma_2 t}}$$

If the time of each dilution step is T, $f = f_0(\frac{e^{\gamma_2 T}+1}{2})^{\frac{\gamma_1-\gamma_2}{\gamma_2}}$. Since $T \gg \frac{1}{\gamma_2}$, we can write that

$f = f_0 e^{(\gamma_1-\gamma_2)Tn}$, where n is the amount of dilution steps.

Length scale in spatial competition.

We consider the following coupled system of Fisher equations:

$$\frac{\partial c_1}{\partial t} = \frac{\partial}{\partial x}(D_1(c)\frac{\partial}{\partial x}c_1) + \gamma_1(c)c_1$$
$$\frac{\partial c_2}{\partial t} = \frac{\partial}{\partial x}(D_2(c)\frac{\partial}{\partial x}c_2) + \gamma_2(c)c_2$$

Where $c = c_1 + c_2$ and c_1 and c_2 are population densities of two competing phenotypes. Growth rates and diffusion constants depend on the total density, because usually they depend on resources abundance. Therefore it is reasonable to assume that the resources abundance is a function of sum of the two densities. We will change the variables of the equations to c and $f = \frac{c_1}{c_1+c_2}$ and assume that$f \ll 1$. Therefore we can neglect higher terms in f in the equation, i. e. linear terms in the equation for total density and quadratic terms in the equation for frequency:

$$\frac{\partial c}{\partial t} = \frac{\partial}{\partial x}(D_2(c)\frac{\partial}{\partial x}c) + \gamma_2(c)c$$
$$\frac{\partial f}{\partial t} = \frac{f}{c}\frac{\partial}{\partial x}((D_1(c) - D_2(c))\frac{\partial}{\partial x}c) + f(\gamma_1(c) - \gamma_2(c)) + \frac{1}{c}\frac{\partial}{\partial x}(D_1(c)c\frac{\partial}{\partial x}f) + \frac{1}{c}\frac{\partial}{\partial x}(D_1(c)f\frac{\partial}{\partial x}c)$$

First equation does not depend on f and has a travelling wave solution with a velocity v.

Switch to the co-moving frame:

D does not depend on c:

$$\frac{\partial f}{\partial t} = D_1\frac{\partial^2}{x^2}f + \frac{2}{c}D_1\frac{\partial}{\partial x}f\frac{\partial}{\partial x}c + \frac{f}{c}(D_1 - D_2)\frac{\partial^2}{x^2}c + f(\gamma_1(c) - \gamma_2(c))$$

$$y = x - v_2 t$$

Linear operator, has the largest eigenvalue that will dominate.

$$\tau = t$$

$$\frac{\partial}{\partial x} = \frac{\partial}{\partial y}$$

$$\frac{\partial}{\partial t} = \frac{\partial}{\partial \tau} - v_2 \frac{\partial}{\partial y}$$

$$\frac{\partial}{\partial y} D_2(c) \frac{\partial}{\partial y} c + v_2 \frac{\partial}{\partial y} c + \gamma_2(c) c = 0$$

$$\frac{\partial f}{\partial \tau} = v_2 \frac{\partial}{\partial y} f + \frac{f}{c} \frac{\partial}{\partial y} ((D_1(y) - D_2(y)) \frac{\partial}{\partial y} c) + f(\gamma_1(c) - \gamma_2(c)) + \frac{1}{c} \frac{\partial}{\partial y} (D_1(y) c \frac{\partial}{\partial y} f)$$
$$+ \frac{1}{c} \frac{\partial}{\partial y} (D_1(y) f) \frac{\partial}{\partial y} c$$

Where $D(y) = D(c(y))$, $c(y)$ is a solution of equation X. The right-hand side of the equation above is a linear operator on f. The long term dynamics of the equation is determined by the largest eigenvalue. $f = e^{-\lambda \tau}$ corresponds to the local decrease of the less fit type. But the wave is moving as a Fisher wave. Therefore, $\frac{\lambda}{v}$ is the corresponding spatial exponent. Let's consider an example – two competing Fisher waves with different growth rates. In this example we will use perturbation theory to find the spatial exponent. As a first step, we will make the operator hermitian by getting rid of the first derivative in y. To do this, we will make a substitution $f(y) = \phi(y) e^{\varphi(y)}$ and choose $\varphi(y)$ such that the coefficient of first derivative of ϕ is 0.

$$\frac{\partial f}{\partial \tau} = D_1 \frac{\partial^2}{\partial y^2} f + \left(v_2 + \frac{2}{c} D_1 \frac{\partial}{\partial y} c\right) \frac{\partial}{\partial y} f + (\gamma_1 - \gamma_2)(1 - c) f$$

$$f(y) = \phi(y) e^{\varphi(y)}$$

$$f' = \phi' e^{\varphi} + \varphi' \phi e^{\varphi(y)}$$

$$f'' = \phi'' e^{\varphi} + 2\varphi' \phi' e^{\varphi(y)} + \varphi'' \phi e^{\varphi(y)} + \varphi'^2 \phi e^{\varphi(y)}$$

$$\frac{\partial \phi}{\partial \tau} = D_1 \phi'' + \left(v_2 + \frac{2}{c} D_1 c' + 2\varphi'\right) \phi' + h(y)\phi + (\gamma_1 - \gamma_2)(1 - c) f$$

Where h(y) – some function of y.

$$\varphi(y) = -\frac{v_2}{2D_1} y - lnc(y)$$

If $\gamma_1 = \gamma_2, f = f_0, \lambda = 0$. Then $\phi_0(y) = f_0 c(y) e^{\frac{v_2}{2D_1} y}$

For not equal growth rates, perturbation theory gives

$$\lambda = 0 + \frac{\int (\gamma_1 - \gamma_2)(1-c) c^2 e^{\frac{v_2}{D_1} y} dy}{\int c^2 e^{\frac{v_2}{D_1} y} dy} = (\gamma_1 - \gamma_2) ,$$

Since we know the scaling of c as y goes to infinity, the second term in (1-c) can be neglected.

Lag time reasoning.

In Fisher model, if one of the strains has spread far enough, the second strain is only left with the diffusion process since the growth rate saturates. In diffusion process, the mean square distance grows linear in time, which means that the effective front of the spread of the second wave will spread as a square root of time. Since the square root has a negative second derivative, there exists a critical lag time when the two curves just touch each other and if the lag time is longer, the second wave will not be able to diffuse though the bulk of the first strain.

Chapter 6

Discussion

In both parts of my thesis, we quantify fitness of populations with complex interactions, i.e. populations in which reproductive ability per unit time is not the metric that is maximized during the selection process. In both examples, there are at least two dimensions that can control fitness and could be varied somewhat independently from each other (V_{max} and K_M for the first example and D and γ for the second example). Diffusion and growth are often negatively correlated. Nevertheless, there are examples when the changes in the values of these parameters violate the general trend and therefore it is at least possible to control them separately. V_{max} and K_M depend collectively of 4 other parameters and can be treated as relatively independent.

Cooperation makes both cases even more complicated – the metric that characterizes performance of the population is not simply the sum of the same metric for an individual. Therefore, the metric of performance of populations will have a different functional dependence on the multiple parameters that determine fitness of the individual. For example, for cooperatively growing bacterial populations in the well-mixed antibiotic environment and the typical parameter values discussed in chapter 2 and 3, V_{max} determines population performance, while V_{max}/K_M determines the fate of an individual. Therefore, it is possible that the population performance becomes worse in the evolutionary process. It will happen if V_{max}/K_M of a new mutant increased while V_{max} decreases.

While cooperation has been discussed in detail only in the well-mixed project, it has interesting consequences for the expanding populations too. Specifically, it is possible that a lower velocity type is selected in expanding populations if the growth is cooperative. Intuitively it can be understood because a slightly slower diffusing type will have a higher tendency to stay around intermediate cell densities and therefore can benefit from the high growth rates which in strongly cooperative cases only happens at intermediate cell densities.

In real life, there could be differences between the desired outcomes (i.e. curing bacterial infection or slowing down expanding population of cane toads) and what evolution maximizes. The worst situation is when they are correlated with coefficient -1. Ideally, they are coinciding or at least orthogonal. In the situations discussed above, cooperation makes it possible for the populations to evolve phenotypes that are beneficial to an individual but make the entire population more vulnerable. While in the extreme example it may force the population to look for non-cooperative mechanisms of growing, often developing those will already decrease the fitness of the population which may solve the problem at hand.

Usually the desired outcomes are at the level of populations – we don't want cane toads to cover new territories, we don't want bacterial infections to get into the blood stream and spread – while evolutionary fitness is maximized on the individual level. Since in many of the real systems we have been discussing there is a negative correlation between individual fitness and probability of desired outcome, our goal must be to use the available knobs to engineer conditions that make this negative correlation as weak as possible or even try to make it positive. As an example of the knob we can consider the strength of cooperation. In general, the viscosity of the media and nutrient concentration can alter the diffusion coefficient and growth rate that are available for the population. The carrying capacity influences the effective population size. Higher effective population sizes let smaller selection coefficients experience selection and not just drift, which should increase their survival chances.

The strength of cooperation could be characterized by measuring how much the performance of the group is different from the performance of the same number of individuals in isolation. Usually, the greater the difference the stronger the cooperation. The result of cooperation usually has the consequence that a group is collectively stronger (together growing faster) than a set of isolated individuals. In cases when the group threatens humans, it has usually negative effects for our health or ecology. On the other hand, there is usually a way to tune the individual performance and the group performance somewhat

separately, which gives a hope to decrease the performance of the group during individual evolution, when every individual maximizes only its own benefit.

One widely discussed example of these dynamics is the spread of cheaters which may individually perform better since they do not pay the cost of cooperation. The higher the cost of cooperation the more incentive there is to cheat. Usually, high costs come with high benefits, otherwise cooperation would not evolve in the first place. Therefore, it is a reasonable assumption that the higher are the cooperative effects in the population, the more room there is to degrade the total fitness of the population by tempting every single individual to cheat. Therefore, it seems reasonable that in some cases increases of the cooperative effects can even further decouple the performance of individuals from performance of the group. And consequently this can result in more ways in which an individual can increase its own fitness, while the fitness of the group is either not affected or decreased.

An extreme example of the ideal result of maximizing the objective function described above would be antibiotic pumps in the first example. Very effective antibiotic pumps minimize antibiotic concentration inside (i.e. maximize fitness of individual), while do not alter the antibiotic concentration in the media (minimize cooperative effect). For the second example, maximization of objective function will result in diffusion coefficient equal to zero in the presence of extreme cooperative growth. While this phenotype will not be fitter on the individual level than any of the diffusing type, selection for small decrease of diffusion does happen at each step. As a result, it is possible by introducing the right mutants at the right time to make diffusion coefficient infinitesimally small.

While it is not always obvious how to restrict access to the mutations that increase both individual benefits and group benefits, one possible experiment is to take pre-existing types and show that under certain conditions they could be selected and at the same time decrease the performance of the population or start many replicates of the evolving populations and post-factum select the strains satisfying this condition. After that, we could compete two genotypes to demonstrate that the competition will select the

decrease of the group performance. With the increase of the genetic engineering methods, introduction of an individual with any pre-defined alleles should not be a problem in the foreseeable future.

References

Ackermann M, Stecher B, Freed NE, Songhet P, Hardt W-D & Doebeli M (2008) Self-destructive cooperation mediated by phenotypic noise. *Nature* **454:** 987–990

Andrews JM (2001) Determination of minimum inhibitory concentrations. *J. Antimicrob. Chemother.* **48:** 5–16

Axelrod R & Hamilton WD (1981) The evolution of cooperation. *Science* **211:** 1390–1396

Barrick JE & Lenski RE (2013) Genome dynamics during experimental evolution. *Nat. Rev. Genet.* **14:** 827–839

Bennett PM (2008) Plasmid encoded antibiotic resistance: acquisition and transfer of antibiotic resistance genes in bacteria. *Br. J. Pharmacol.* **153:** S347–S357

Björkman J, Nagaev I, Berg OG, Hughes D & Andersson DI (2000) Effects of environment on compensatory mutations to ameliorate costs of antibiotic resistance. *Science* **287:** 1479–1482

Bonomo RA & Tolmasky M (2007) Enzyme-mediated resistance to antibiotics : mechanisms, dissemination, and prospects for inhibition Washington, D.C.: ASM Press

Brook I (1989) Inoculum effect. *Rev. Infect. Dis.* **11:** 361

Brown JE, Del Bene VE & Collins CD (1981) In vitro activity of N-formimidoyl thienamycin, moxalactam, and other new beta-lactam agents against Bacteroides fragilis: contribution of beta-lactamase to resistance. *Antimicrob. Agents Chemother.* **19:** 248–252

Bush K, Jacoby GA & Medeiros AA (1995) A functional classification scheme for beta-lactamases and its correlation with molecular structure. *Antimicrob. Agents Chemother.* **39:** 1211

Chadwick P (1966) Field trial of a microcolony method for testing the antibiotic sensitivity of bacteria. *Can. Med. Assoc. J.* **95:** 852

Chung HS, Yao Z, Goehring NW, Kishony R, Beckwith J & Kahne D (2009) Rapid β-lactam-induced lysis requires successful assembly of the cell division machinery. *Proc. Natl. Acad. Sci.* **106:** 21872–21877

Clark DR, Alton TM, Bajorek A, Holden P, Dugatkin LA, Atlas RM & Perlin MH (2009) Evolution of altruists and cheaters in near-isogenic populations of Escherichia coli. *Front. Biosci. J. Virtual Libr.* **14:** 4815

Clinical & Institute LS (2009) Performance Standards for Antimicrobial Susceptibility Testing of Anaerobic Bacteria: Informational Supplement Clinical and Laboratory Standards Institute

CLSI document M07-A9 (2012) Methods for Dilution Antimicrobial Susceptibility Tests for Bacteria That Grow Aerobically; Approved Standard—Ninth Edition.

Cowen LE, Kohn LM & Anderson JB (2001) Divergence in fitness and evolution of drug resistance in experimental populations of Candida albicans. *J. Bacteriol.* **183:** 2971–2978

Demanèche S, Sanguin H, Poté J, Navarro E, Bernillon D, Mavingui P, Wildi W, Vogel TM & Simonet P (2008) Antibiotic-resistant soil bacteria in transgenic plant fields. *Proc. Natl. Acad. Sci.* **105:** 3957–3962

Dugatkin LA, Perlin M, Lucas JS & Atlas R (2005) Group-beneficial traits, frequency-dependent selection and genotypic diversity: an antibiotic resistance paradigm. *Proc. R. Soc. B Biol. Sci.* **272:** 79–83

Ewbank JJ & Zugasti O (2011) C. elegans: model host and tool for antimicrobial drug discovery. *Dis. Model. Mech.* **4:** 300–304

Fisher RA (1937) The Wave of Advance of Advantageous Genes. *Ann. Eugen.* **7:** 355–369

Goldstein EJ, Citron DM & Cherubin CE (1991) Comparison of the inoculum effects of members of the family Enterobacteriaceae on cefoxitin and other cephalosporins, beta-lactamase inhibitor combinations, and the penicillin-derived components of these combinations. *Antimicrob. Agents Chemother.* **35:** 560–566

Gullberg E, Cao S, Berg OG, Ilbäck C, Sandegren L, Hughes D & Andersson DI (2011) Selection of resistant bacteria at very low antibiotic concentrations. *Plos Pathog.* **7:** e1002158

Hadeler KP & Rothe F (1975) Travelling fronts in nonlinear diffusion equations. *J. Math. Biol.* **2:** 251–263

Hall BG (2002) Predicting evolution by in vitro evolution requires determining evolutionary pathways. *Antimicrob. Agents Chemother.* **46:** 3035–3038

Hallatschek O & Nelson DR (2010) Life at the Front of an Expanding Population. *Evolution* **64:** 193–206

Hermsen R, Deris JB & Hwa T (2012) On the rapidity of antibiotic resistance evolution facilitated by a concentration gradient. *Proc. Natl. Acad. Sci.* **109:** 10775–10780

Jacoby GA (2006) β-Lactamase Nomenclature. *Antimicrob. Agents Chemother.* **50:** 1123–1129

Johnson PJT & Levin BR (2013) Pharmacodynamics, Population Dynamics, and the Evolution of Persistence in Staphylococcus aureus. *Plos Genet* **9:** e1003123

Kolmogorov AN, Petrovskii IG & Piskunov NS (1937) A study of the equation of diffusion with increase in the quantity of matter, and its application to a biological problem. *Bjul Mosk. Gos Univ*: 1–26

Leclercq R (2002) Mechanisms of Resistance to Macrolides and Lincosamides: Nature of the Resistance Elements and Their Clinical Implications. *Clin. Infect. Dis.* **34:** 482–492

Lee HH, Molla MN, Cantor CR & Collins JJ (2010) Bacterial charity work leads to population-wide resistance. *Nature* **467:** 82–85

Madigan MT, Martinko JM, Dunlap PV & Clark DP (2009) Brock biology of microorganisms Pearson/Benjamin Cummings

Martínez JL (2008) Antibiotics and Antibiotic Resistance Genes in Natural Environments. *Science* **321:** 365–367

Mohan R, Mukherjee A, Sevgen SE, Sanpitakseree C, Lee J, Schroeder CM & Kenis PJA (2013) A multiplexed microfluidic platform for rapid antibiotic susceptibility testing. *Biosens. Bioelectron.* **49:** 118–125

Moy TI, Ball AR, Anklesaria Z, Casadei G, Lewis K & Ausubel FM (2006) Identification of novel antimicrobials using a live-animal infection model. *Proc. Natl. Acad. Sci.* **103:** 10414–10419

Negri M-C, Lipsitch M, Blázquez J, Levin BR & Baquero F (2000) Concentration-Dependent Selection of Small Phenotypic Differences in TEM β-Lactamase-Mediated Antibiotic Resistance. *Antimicrob. Agents Chemother.* **44:** 2485–2491

Nikaido H & Normark S (1987) Sensitivity of Escherichia coli to various beta-lactams is determined by the interplay of outer membrane permeability and degradation by periplasmic beta-lactamases: a quantitative predictive treatment. *Mol. Microbiol.* **1:** 29–36

Normark BH & Normark S (2002) Evolution and spread of antibiotic resistance. *J. Intern. Med.* **252:** 91–106

Nowak MA (2006) Five rules for the evolution of cooperation. *Science* **314:** 1560–1563

Paulander W, Pennhag A, Andersson DI & Maisnier-Patin S (2007) Caenorhabditis elegans as a Model To Determine Fitness of Antibiotic-Resistant Salmonella enterica Serovar Typhimurium. *Antimicrob. Agents Chemother.* **51:** 766–769

Philippon A, Labia R & Jacoby G (1989) Extended-spectrum beta-lactamases. *Antimicrob. Agents Chemother.* **33:** 1131

Phillips BL, Brown GP, Webb JK & Shine R (2006) Invasion and the evolution of speed in toads. *Nature* **439:** 803–803

Rapid antibiotic susceptibility testing by tracking single cell growth in a microfluidic agarose channel system - Lab on a Chip (RSC Publishing) *Lab. Chip*

Shaw KJ, Rather PN, Hare RS & Miller GH (1993) Molecular genetics of aminoglycoside resistance genes and familial relationships of the aminoglycoside-modifying enzymes. *Microbiol. Rev.* **57:** 138–163

Soong J & Soni N (2012) Sepsis: recognition and treatment. *Clin. Med.* **12:** 276–280

Stemmer WPW (1994) Rapid evolution of a protein in vitro by DNA shuffling. *Nature* **370:** 389–391

Stiernagle T (2006) Maintenance of C. elegans. *WormBook*

Sykes RB & Matthew M (1976) The β-lactamases of Gram-negative bacteria and their rôle in resistance to β-lactam antibiotics. *J. Antimicrob. Chemother.* **2:** 115–157

Tan C, Phillip Smith R, Srimani JK, Riccione KA, Prasada S, Kuehn M & You L (2012) The inoculum effect and band-pass bacterial response to periodic antibiotic treatment. *Mol. Syst. Biol.* **8:**

Tan L, Serene S, Chao HX & Gore J (2011) Hidden randomness between fitness landscapes limits reverse evolution. *Phys. Rev. Lett.* **106:** 198102

Tanouchi Y, Pai A, Buchler NE & You L (2012) Programming stress-induced altruistic death in engineered bacteria. *Mol. Syst. Biol.* **8:**

Templeton AR (2002) Out of Africa again and again. *Nature* **416:** 45

Walsh C (2000) Molecular mechanisms that confer antibacterial drug resistance. *Nature* **406:** 775–781

Wang X, Minasov G & Shoichet BK (2002) Evolution of an antibiotic resistance enzyme constrained by stability and activity trade-offs. *J. Mol. Biol.* **320:** 85–95

Weinreich DM, Delaney NF, DePristo MA & Hartl DL (2006) Darwinian evolution can follow only very few mutational paths to fitter proteins. *Science* **312:** 111–114

Wiegand I, Hilpert K & Hancock REW (2008) Agar and broth dilution methods to determine the minimal inhibitory concentration (MIC) of antimicrobial substances. *Nat. Protoc.* **3:** 163–175

Wiser MJ, Ribeck N & Lenski RE (2013) Long-Term Dynamics of Adaptation in Asexual Populations. *Science* **342:** 1364–1367

Wiuff C, Zappala RM, Regoes RR, Garner KN, Baquero F & Levin BR (2005) Phenotypic Tolerance: Antibiotic Enrichment of Noninherited Resistance in Bacterial Populations. *Antimicrob. Agents Chemother.* **49:** 1483–1494

Yao Z, Kahne D & Kishony R (2012) Distinct Single-Cell Morphological Dynamics under Beta-Lactam Antibiotics. *Mol. Cell* **48:** 705–712

Yeh PJ, Hegreness MJ, Aiden AP & Kishony R (2009) Drug interactions and the evolution of antibiotic resistance. *Nat. Rev. Microbiol.* **7:** 460–466

Yurtsev EA, Chao HX, Datta MS, Artemova T & Gore J (2013) Bacterial cheating drives the population dynamics of cooperative antibiotic resistance plasmids. *Mol. Syst. Biol.* **9:** Available at: http://msb.embopress.org/content/9/1/683.abstract [Accessed November 3, 2014]

Zimmermann W & Rosselet A (1977) Function of the outer membrane of Escherichia coli as a permeability barrier to beta-lactam antibiotics. *Antimicrob. Agents Chemother.* **12:** 368–372